

**Boise State University**  
**ScholarWorks**

---

Geosciences Faculty Publications and Presentations

Department of Geosciences

---

2-2-2010

# High-Precision U-Pb Zircon Age Calibration of the Global Carboniferous Time Scale and Milankovitch Band Cyclicity in the Donets Basin, Eastern Ukraine

Vladimir I. Davydov  
*Boise State University*

James L. Crowley  
*Boise State University*

Mark D. Schmitz  
*Boise State University*

Vladislav I. Poletaev  
*Ukrainian Academy of Sciences*



## High-precision U-Pb zircon age calibration of the global Carboniferous time scale and Milankovitch band cyclicality in the Donets Basin, eastern Ukraine

Vladimir I. Davydov, James L. Crowley, and Mark D. Schmitz

*Department of Geosciences, Boise State University, Boise, Idaho 83725, USA (markschmitz@boisestate.edu)*

Vladislav I. Poletaev

*Department of Paleontology and Stratigraphy, Institute of Geological Science, Ukrainian Academy of Sciences, 55 Gonchar Street, Kiev 252601, Ukraine*

[1] High-precision ID-TIMS U-Pb zircon ages for 12 interstratified tuffs and tonsteins are used to radiometrically calibrate the detailed lithostratigraphic, cyclostratigraphic, and biostratigraphic framework of the Carboniferous Donets Basin of eastern Europe. Chemical abrasion of zircons, use of the internationally calibrated EARTHTIME mixed U-Pb isotope dilution tracer, and improved mass spectrometry guided by detailed error analysis have resulted in an age resolution of <0.05%, or ~100 ka, for these Carboniferous volcanics. This precision allows the resolution of time in the Milankovitch band and confirms the long-standing hypothesis that individual high-frequency Pennsylvanian cyclothem and bundles of cyclothem into fourth-order sequences are the eustatic response to orbital eccentricity (~100 and 400 ka) forcing. Tuning of the fourth-order sequences in the Donets Basin to the long-period eccentricity cycle results in a continuous age model for the Middle to Late Pennsylvanian (Moscovian-Kasimovian-Ghzelian) strata of the basin and their record of biological and climatic changes through the latter portion of the late Paleozoic Ice Age. Detailed fusulinid and conodont zonations allow the export of this age model to sections throughout Euramerica. Additional ages for Mississippian strata provide among the first robust radiometric calibration points within this subperiod and result in variable lowering of the base ages of its constituent stages compared to recent global time scale compilations.

**Components:** 15,187 words, 7 figures, 2 tables.

**Keywords:** U-Pb geochronology; zircon; Carboniferous; time scale; cyclostratigraphy; biostratigraphy.

**Index Terms:** 1115 Geochronology: Radioisotope geochronology; 1135 Geochronology: Correlative geochronology; 4946 Paleoclimatology: Milankovitch theory.

**Received** 9 July 2009; **Revised** 26 October 2009; **Accepted** 13 November 2009; **Published** 2 February 2010.

Davydov, V. I., J. L. Crowley, M. D. Schmitz, and V. I. Poletaev (2010), High-precision U-Pb zircon age calibration of the global Carboniferous time scale and Milankovitch band cyclicality in the Donets Basin, eastern Ukraine, *Geochem. Geophys. Geosyst.*, 11, Q0AA04, doi:10.1029/2009GC002736.

**Theme:** EarthTime: Advances in Geochronological Technique

**Guest Editors:** D. Condon, G. Gehrels, M. Heizler, and F. Hilgen

## 1. Introduction

[2] The Donets Basin of eastern Europe contains one of the most complete global Carboniferous sedimentary successions, with few gaps in its depositional record [Aisenverg *et al.*, 1975; Davydov, 1990; Fohrer *et al.*, 2007]. These marine to paralic strata of the Donets Basin host over 250–300 limestones and about 250 coal horizons [Aisenverg *et al.*, 1963, 1971; Levenshtein, 1963] and thus contain exceptionally well-established marine invertebrate and terrestrial floral biostratigraphic records, which are important standards for global marine and continental correlation. Many of the faunal indexes now considered for the Carboniferous time scale (i.e., foraminifera *Eoparastaffella simplex* for the base of the Viséan [Vdovenko, 1954], *Protriticites pseudomontiparus* [Putrja, 1948] and *Obsoletes obsoletus* [Schellwien, 1908] for the traditional base of the Kasimovian, and *Rauserites rossicus* for the base of the Gzhelian [Davydov *et al.*, 2008; Schellwien, 1908]; and conodonts *Declinagnathodus donetzianus* for the base of the Moscovian and *Idiognathodus sagittalis* for the recently considered higher base of the Kasimovian [Kozitskaya *et al.*, 1978; Nemyrovskaya *et al.*, 1999]) were originally recognized and described from the Donets Basin. The paleogeography of the Donets Basin lends particular importance to these records, in that they provide a linchpin for pan-Euramerican continental-marine biostratigraphic correlation. Moreover, deposition in this paralic setting appears to have kept pace with rapid basin subsidence, such that Donets Basin strata were eustatically responsive and exceptionally cyclic [Zhemchuzhnikov and Yablokov, 1956]. The basin has been recently reinterpreted in terms of modern sequence stratigraphy [Briand *et al.*, 1998; Izart *et al.*, 1996; Izart *et al.*, 2003], leading to a proposed hierarchy of fourth-order and higher-frequency cycles.

[3] The detailed lithostratigraphy and biostratigraphy of the Donets Basin, combined with an abundance of interstratified volcanic layers provide a unique opportunity for precise radiometric calibration of the basin's cyclostratigraphic and chronostratigraphic framework. Volcanic horizons, including limestone-hosted altered K-bentonites and coal-hosted tonsteins, have been recognized in the Donets Basin successions for over 50 years [Chernov'yants, 1992]. However, prior attempts at  $^{40}\text{Ar}/^{39}\text{Ar}$  dating of tonsteins [Hess *et al.*, 1999] produced problematic results, suggesting apparent discrepancies of 5–6 Ma between traditionally correlated faunas of the Donets Basin, western

Europe, and the Appalachian Basin of North America. Recent advances in U-Pb zircon geochronology utilizing the isotope dilution thermal ionization mass spectrometry (ID-TIMS) method can now provide radiometric age constraints for late Paleozoic samples exceeding 0.05% age resolution [Ramezani *et al.*, 2007]. We collected samples of coal tonstein and altered volcanic ash from throughout the Carboniferous succession of the Donets Basin with the goal of using high-precision U-Pb zircon geochronology to refine its chronostratigraphic framework, test for Milankovitch band orbital controls on cyclic sedimentation, and calibrate biostratigraphic zonations integral to the construction of a high-resolution global time scale.

## 2. Geologic and Stratigraphic Context

### 2.1. Geologic Setting

[4] The Donets Basin is the southeastern segment of the Dniepr–Donets Depression (Figure 1), a Late Devonian rift structure located on the southern rampart of the eastern European craton [Stovba and Stephenson, 1999]. The Donets Basin plunges beneath Upper Cretaceous sediments to the southeast, gradually giving way to the Karpinsky Swell, which borders the Pre-Caspian syncline in the north and east, and the Scythian Platform to the south. Sediment thicknesses (comprising Silurian–Devonian prerift and synrift and Carboniferous–Palaeogene postrift successions) increase from about 2 km in the central and westernmost Dniepr–Donets Depression to about 22 km in the Donets Basin [Chekunov, 1994; Stovba *et al.*, 1996]. The Donets Basin is generally considered to have been profoundly uplifted during the Early Permian in response to the buildup of stresses emanating from the Hercynian–Caucasus–Uralian orogens [Milanovsky, 1992] or to the activity of an asthenospheric mantle diapir [Chekunov, 1994; Gavrish, 1989]. The folded and exposed portion of the Donets Basin is often termed the “Open Donbass,” while the major portion of the basin covered by Cretaceous and younger sediments is referred to as the “Covered Donbass”; together they form the so-called “Greater Donbass.”

### 2.2. Biostratigraphic Zonation

[5] Paleontological and biostratigraphic studies in the Donets Basin were always a priority of overall geological exploration in the basin. All major fossil groups have been studied and many are thoroughly

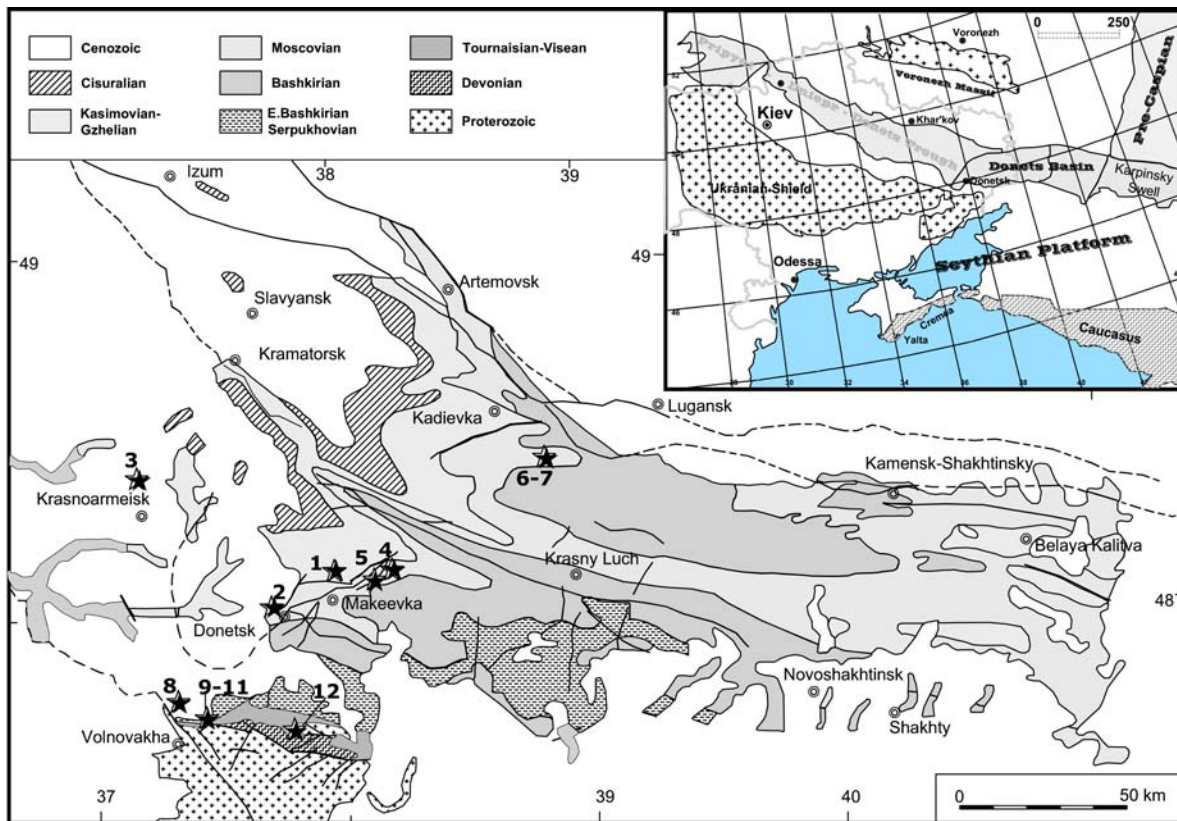


**Figure 1.** Location map of the Donets Basin including major tectonic elements and sampling sites, modified from Aizenverg *et al.* [1975].

described. Brachiopods have been studied since the 19th century as they were widely used until the 1950s for intrabasinal correlation; a local brachiopod zonation has been proposed for Carboniferous strata of the Donets Basin [Kagarmanov and Donakova, 1990; Vdovenko *et al.*, 1990]. Ammonooids are another group of classical fossils that are rare in the Donets Basin, but well studied [Aizenverg *et al.*, 1979; Popov, 1979]. They are best used for characterizing the Serpukhovian-Bashkirian portions of the succession, and to a lesser degree the Moscovian and mid-Visean, providing effective correlation with classical ammonoid successions in Great Britain and Germany.

[6] Foraminifers were the primary chronostratigraphic tool for subdivision and correlation of Carboniferous strata within the entire Dnieper-Donets trough as well as with other regions including the Russian Platform and Urals, western Europe, and central Asia [Brazhnikova *et al.*, 1967; Davydov, 1990; Kireeva, 1951; Vdovenko, 2001]. Overall, 38 foraminiferal zones (Figure 2) are established for the entire Carboniferous with an average duration of 1.5–2.0 Ma (but sometimes up to 6 Ma). Foraminifers provided direct correlation

of the Donets Basin succession with type sections of the Mississippian in Belgium [Cozar *et al.*, 2008; Devuyt *et al.*, 2003; Devuyt and Kalvoda, 2007; Poty *et al.*, 2006; Vdovenko, 2001] and Pennsylvanian type sections in the Moscow Basin and Urals [Aizenverg *et al.*, 1983].

[7] Conodonts are locally abundant in the Carboniferous of the Donets Basin, but have been studied only since the late 1970s [Kozitskaya *et al.*, 1978]. Study has focused in the Bashkirian, Moscovian and lower Kasimovian portions of the successions [Fohrer *et al.*, 2007; Nemyrovskaya, 1999; Nemyrovskaya *et al.*, 1999]. Conodonts provide reasonable correlation in the Mississippian and Late Pennsylvanian, and an excellent zonation and correlation for early Middle Pennsylvanian (Figure 2), although they are quite provincial in the middle Moscovian [Goreva and Alekseev, 2007].

[8] Other abundant and well studied fossils in the Carboniferous of the Donets Basin (corals, trilobites, bivalves, bryozoans, ostracods, plants and miospores) are used only for local and regional correlation and paleoecological interpretations. Among them plants and miospores recovered in



**Figure 2.** Chronostratigraphic scale for the Donets Basin [Davydov, 2009; Davydov and Khodjanyazova, 2009; Nemyrovska, 1999; Nemyrovska et al., 1999; Poletaev, 1981; Poletaev et al., 1991] and correlation chart to regional stages of the Russian Platform/Ural, western Europe [Poty et al., 2006], and North America [Davydov et al., 2004; Wardlaw et al., 2004].



the Donets Basin are important for correlation of marine sequences with entirely continental Middle-Late Pennsylvanian and Permian deposits in western Europe and the Appalachian Basin in North America [Fisunenko, 2000; Inosova et al., 1976; Shchegolev, 1975; Shchegolev and Kozitskaya, 1984].

### 2.3. Stratigraphic Nomenclature

[9] The Donets Basin as a major coal basin in Ukraine has been explored and studied since the 18th century. Its territory is mapped in great detail (mostly at 1:25000 scale, with major coal production areas at 1:5000 scale on an instrumental basis) with many sections measured and several thousand wells drilled and studied from different perspectives [Rotai, 1975]. The late Paleozoic succession can be conveniently divided into three parts. The lower part is an approximate analog to the Dinantian of western Europe (latest Devonian-Tournaisian to Viséan) and consists of shallow shelf to midramp carbonates formed in a subplatform setting. The middle and the thickest part of the succession (Serpukhovian through early Gzhelian) consists of paralic, cyclic intercalations of siliciclastics (97% of succession) and thin layers of shallow limestone (2% of succession) usually less than 1 m thick, but sometimes up to 5–10 m thick. Coals represent about 1% of this middle succession and average 0.3–0.5 m in thickness, but are sometimes up to 2 m thick. The upper part of the succession comprises late Gzhelian-Asselian continental siliciclastic red beds with a very few and thin marine incursions; this upper portion of the succession is not considered further here.

[10] Early workers [Lebedev, 1924; Lutugin and Stepanov, 1913; Tschernyshev and Lutugin, 1897] divided the entire succession into a series of Formations named with digital indexes and/or Latin letters. The traditional Russian and then USSR tripartite system for Carboniferous subdivisions is used in the Donets Basin. The lower “Dinantian” portion of the succession, totaling nearly 500 m of limestone, is named as the Mokrovolnovakhsкая Series with the index  $C_1^1$  (A), and includes ten formations. These formations possess a parallel biostratigraphic zone indexing of the form  $C_1^1a$  through  $C_1^1d$ , and  $C_1^1a$  through  $C_1^1f$ .

[11] The middle cyclic succession is divided into 15 formations [ $C_1^2$  (B),  $C_1^3$  (C) etc.], each with specific names (i.e., Isaevskaya, Araukaritovaya, etc.). The beginning of each formation usually starts with a thick limestone representing the be-

ginning of a major transgressive cycle. Within each formation the number of limestone bands varies from four ( $C_2^4$  (I) Formation) to forty ( $C_1^4$  (D) Formation). The number of limestone bands in each formation and their thickness changes laterally because of the transgressive-regressive character of cycles [Aisenverg et al., 1975]. Specifically, the number of limestone bands and their thickness increases eastward toward the deepest part of the Donets Basin and the Precaspian Basin. These marine bands are designated by capital letters with subscript and superscript numerals (Figure 2). Major limestones within each formation that can be traced throughout the basin are integered with a subscript numeral from oldest to youngest; minor limestones between these major bands are labeled with the major subscript and an additional superscript signifying its order between major bands. For example,  $D_5^1$  signifies the seventh minor limestone between the fifth and sixth major limestone bands, from the base of the  $C_1^4$  (D) formation. A similar nomenclature was proposed for the coal seams, with a lowercase letter and additional subscript and superscript numbers such as  $h_5^1$ , i.e., the same system of divisions of major and minor coals. The majority of coals appear beneath limestones, indicating the beginning of transgression.

[12] It is generally accepted that most of the major limestones and coals extended laterally throughout the basin and form a comprehensive stratigraphic framework. Lutugin and Stepanov [1913] proposed to use both limestone and coals as lateral marker beds, i.e., as isochronous horizons, for mapping. “Lutugin’s” system is still widely used in the Donets Basin as a chronostratigraphic tool in mapping and correlation. However, Davydov [1992] reported that the same limestone can change its apparent biochronology laterally, at least up to one biostratigraphic zone and therefore it cannot be excluded that at least some limestones are slightly diachronous throughout the basin, although some of the authors of this paper (VIP) do not support this idea.

### 2.4. Lithostratigraphy

[13] Given the importance of the stratigraphic positioning and reproducibility of the high-precision radiometric ages reported in this paper, the lithostratigraphic and biostratigraphic architecture of the Donets Basin is described in the auxiliary material.<sup>1</sup> That discussion provides a detailed stratigraphic context whose description has hitherto been pre-

<sup>1</sup>Auxiliary materials are available in the HTML. doi:10.1029/2009GC002736.

dominantly restricted to Russian and Ukrainian languages literature. In that discussion we further highlight the biostratigraphic correlations of the Donets Basin strata with their equivalents in the Russian Platform and western Europe and in order to illuminate how our new radiometric ages may be exported outside of the Donets Basin to constrain the global time scale (Figure 2).

### 3. Carboniferous Global Chronostratigraphy

[14] The conodont species *Siphonodella praesulcata* and *S. sulcata* are two indexes that designate the base of the Carboniferous (Tournaisian Stage) in the global scale [Davydov et al., 2004]. The base of the Tournaisian Stage in the Donets Basin is therefore located between: the late Devonian Porfirytovaya Formation with foraminifera *Quasiendothyra* ex gr. *communis* (Rauser), Q. ex gr. *kobeitusana* (Rauser), Q. ex gr. *konensis* (Lebedeva), *Cribrosphaeroides* sp., *Paracaligelloides tlourennensis* Conil et Lys, *Tournayella* sp., *Septatournayella* sp., *Septaglomospiranella* sp., *Septabrunciina* sp., and the index conodont *Siphonodella praesulcata* Sandberg; and the early Tournaisian Bazalievskaya Formation, which contains foraminifera *Bisphaera malevkensis* Birina, *Septaglomospiranella* spp. and *Earlandia minima* Birina, and conodonts *Siphonodella* aff. *sulcata* (Huddle), *S. semichatovae* Kononova and Lipnjagov, *Patrog-nathus andersoni* Klapper. An unconformity at the base of Basalievskaya Formation [Poletaev, 1981; Poletaev et al., 1991] is most probably insignificant.

[15] The base of the global Visean Stage was recently defined at the base of bed 85 of the Pengchong section in Guangxi, south China by the first appearance of the foraminifera *Eoparastaffella simplex* in the lineage *Eoparastaffella ovalis*–*Eoparastaffella simplex* [Devuyst et al., 2003]. Both species were originally described from the Donets Basin [Vdovenko, 1954] along with other latest Tournaisian and early Visean foraminifera. The first appearance datum (FAD) of *Eoparastaffella simplex* in the Donets Basin and consequently the base of the global Visean Stage therefore appears at the base of the Skelevatskaya Formation, or biostratigraphic zone C<sub>1</sub><sup>y</sup>b [Vdovenko, 2001].

[16] The base of the Serpukhovian Stage in the global time scale is not yet officially established, however the conodont species *Lochrea zieglerei* has been proposed as an index [Nemirovskaya et al.,

1994; Skompski et al., 1995]. The occurrence of this species is reported in late Visean Brigantian Stage in north England, in the gamma *Goniatites* or *Emsitites shaelkensis* goniatite zone of the Rheinisches Schiefergebirge of Germany, in the south of the Brousset Valley (Cretes de Soques, Tourmont) of France, in the middle to late Venevian Horizon in Moscow Basin [Skompski et al., 1995], from the late Visean in the Cantabrian Mountains in Spain [Belka and Lehmann, 1998]; together with ammonoids *Lusitanoceras* and *Donbarites falcatoides mirousei* Kullmann (middle Brigantian, late Visean) in the Pyrenees Occidentales [Kullmann et al., 2008], and in the late Visean Hypergoniatites-Ferganoceras ammonoid zone of the Dombar Hills of the southern Urals [Nikolaeva et al., 2009; Kulagina et al., 2006]. Therefore, the proposed boundary is located in the middle to upper part of the Brigantian stage of western Europe and in the middle Venevian Horizon of the Moscow Basin [Davydov et al., 2004]. The analogs of the Venevian Horizon in the Donets Basin are two biostratigraphic foraminiferal zones: the upper part of the *Betpakodiscus compressus* zone (B<sub>4</sub>–B<sub>5</sub> limestones) and the *Euxinita efremovi* zone (B<sub>5</sub>–B<sub>12</sub> limestones). The proposed base of the global Serpukhovian Stage in Donets Basin could be conventionally placed somewhere around the B<sub>9</sub> limestone (uppermost C<sub>1</sub><sup>y</sup>g<sub>1</sub> biostrat. zone). However, it cannot be excluded that the boundary might be placed as low as the B<sub>5</sub> or B<sub>1</sub> limestone because of the occurrence of *Janischevskina* and *Cimmacamina* in the top of the Donetskaya Formation [Vdovenko, 2001]. Both taxa are considered to be diagnostic for the late Brigantian in western Europe [Poty et al., 2006; Somerville, 2008] from which *Lochrea zieglerei* is reported (see above).

[17] The Mid-Carboniferous boundary or the base of the global Bashkirian Stage in the Donets Basin can be placed very precisely. The Kalmius section has an excellent fossil record of the Serpukhovian-Bashkirian transition [Aizenverg et al., 1983] and has been proposed as a candidate GSSP for the boundary [Nemirovskaya et al., 1990]. Exceptionally well-studied conodonts and foraminifera both precisely indicate the position of the boundary. The FAD of the conodont index for the mid-Carboniferous boundary, *Declinognathodus noduliferus*, is in the D<sub>5</sub><sup>8</sup> upper limestone [Nemyrovskaya, 1999], at the base of the C<sub>1</sub><sup>n</sup>d<sub>2</sub> or C<sub>1</sub><sup>s</sup>g biostratigraphic zone. Foraminifera *Plectostaffella bogdanovkensis* Reitlinger and *Millerella umbilicata* Kireeva appear slightly below, in the D<sub>5</sub><sup>7</sup> limestone [Aizenverg et al., 1983].



[18] The base of the Moscovian Stage in the Moscow Basin has been recently redefined on the basis of foraminifers *Aljutovella aljutovica* (Rauser) and *Schubertella pauciseptata* Rauser [Makhlina et al., 2001] at the base of the marine Aljutovo Formation, slightly above the traditional position [Rauser-Chernousova and Reitlinger, 1954]. Foraminiferal workers place the base of Moscovian in the Donets Basin either at the I<sub>2</sub> limestone [Grozdilova, 1966], at the K<sub>1</sub> limestone [Kireeva, 1951], or up to the K<sub>3</sub> limestone where *Aljutovella aljutovica* (Rauser) was first reported [Aisenverg et al., 1963]. Our recent study shows the transitional character of foraminiferal evolution within the I<sub>2</sub> to K<sub>3</sub> limestone sequences with the appearance of fusulinids of the *Aljutovella aljutovica* (Rauser) group as low as the I<sub>2</sub> limestone [Khodjanyazova and Davydov, 2008]. The conodont species *Declinognathodus donetzianus* designated from Donets Basin [Nemyrovska, 1999] has been proposed as an index of the base of the global Moscovian Stage. The FAD of this species in Donets Basin is at the K<sub>1</sub> limestone and thus closely coincides with the traditional lower boundary of the Moscovian Stage in the Moscow Basin [Pazukhin et al., 2006]. Conodont *Diplognathodus ellesmerensis* Bender, recently proposed as another potential index for the base of the global Moscovian Stage [Wang et al., 2007], appears in the Donets Basin at the K<sub>3</sub> limestone [Nemyrovska et al., 1999]. The Bashkirian-Moscovian boundary is provisionally placed at the K<sub>1</sub> limestone in accordance with its historical position in the type area of the Moscow Basin.

[19] The biostratigraphic marker for the traditional base of the Kasimovian Stage in the Moscow Basin is the base of the fusulinid zone *Protriticetes pseudomontiparus-Obsoletus obsoletes* [Ivanova and Khvorova, 1955; Kabanov et al., 2006; Rauser-Chernousova and Reitlinger, 1954]. Both foraminiferal indexes of this zone were originally described from the Donets Basin [Putrja, 1948; Schellwien, 1908], however the range of the first species in the Donets Basin is debated. In our current investigation it has been found in the N<sub>3</sub> and N<sub>5</sub> limestones [Khodjanyazova and Davydov, 2008]. The second species occurs in the Donets Basin in the N<sub>5</sub><sup>1</sup> and O<sub>1</sub> limestones [Davydov, 1992]. Similarly, the index of the traditional lower Kasimovian conodont zone *Streptognathodus subexcelsus* Alekseev and Goreva [Alekseev and Goreva, 2006] has been found in the Moscow Basin in the lithological unit “sharsha” in the lower part of

Suvorovskaya Formation, and in the N<sub>3</sub> limestone of the Donets Basin [Nemyrovska, 1999].

[20] This traditional base of the Kasimovian Stage has not been accepted by the Subcommittee on Carboniferous Stratigraphy Working Group to establish the global Moscovian-Kasimovian boundary. The currently proposed index for the boundary is the conodont species *Idiognathodus sagittalis* Kozitskaya [Villa and the Task Group, 2008]. This species has been described from the O<sub>1</sub> limestone in the Donets Basin [Kozitskaya et al., 1978] and from the upper Neverovo Formation in the middle Kasimovian of the Moscow Basin [Alekseev and Goreva, 2006]. This level is slightly above the FAD of the fusulinid genus *Montiparus* in the Moscow Basin [Davydov, 1997]. The newly proposed boundary therefore occurs approximately in the Middle Kasimovian in the traditional sense [Ivanova and Khvorova, 1955].

[21] Historically, the base of the Gzhelian Stage has been defined in the Moscow Basin at the base of the Rusavkino Formation [Nikitin, 1890] by the first appearance of fusulinid species *Rauserites rossicus* (Schellwien) and *R. stuckenbergi* (Rauser) [Rauser-Chernousova, 1941; Rozovskaya, 1950]. *Rauserites rossicus* was originally described from two areas, from the upper Rusavkino Formation near Gzhel village and from an unspecified limestone from the upper part of the Avilovskaya Formation [Schellwien, 1908]. The specimens from the upper Rusavkino Formation have been designated as a new subspecies *Rauserites rossicus gzhelicus* (Bensh) [Isakova and Ueno, 2007], and similar forms from the Donets Basin as the subspecies *Rauserites rossicus rossicus* (Schellwien) [Davydov et al., 2008]. The base of the Gzhelian Stage exposed near Gzhel village, however, coincides with an unconformity [Makhlina et al., 1979]. In the type location near the Gzhel village only *R. rossicus gzhelicus* (Bensh) and *R. stuckenbergi* have been recovered from the upper Rusavkino Fm. [Davydov et al., 2008]. In the Donets Basin fusulinids of the *Rauserites rossicus* group have been reported from the O<sub>4</sub><sup>1</sup> and O<sub>4</sub><sup>2</sup>, O<sub>5</sub>, O<sub>6</sub><sup>1</sup> and O<sub>7</sub> limestones [Davydov, 1992]. Further study of the fusulinids from O<sub>4</sub><sup>1</sup>, O<sub>4</sub><sup>2</sup>, O<sub>5</sub> and O<sub>6</sub><sup>1</sup> limestones have led to their designation as new and more primitive representatives than *Rauserites rossicus*. Species *Rauserites rossicus rossicus* (Schellwien) has been found only in the O<sub>7</sub> limestone [Davydov et al., 2008; Isakova and Ueno, 2007].





[22] The conodont species *Streptognathodus simulator* [Ellison, 1941] has been proposed as the index to define the base of the global Gzhelian Stage [Chernykh et al., 2006; Heckel et al., 2008]. This species was originally described from the Heebner Shale Member of the Oread limestone [Ellison, 1941] in the midcontinent of North America, and has been widely used as a marker for the boundary in the Moscow Basin [Barskov and Alekseyev, 1975] and in the Urals [Chernykh and Reshetkova, 1987; Chernykh, 2002; Davydov and Popov, 1991]. Barrick et al. [2004, 2008] have proposed a taxonomic revision at the generic level to *Idiognathodus simulator*, although this change is not universally recognized [Chernykh, 2005], nor is its ancestry definitively established. We have retained the original generic name of *Ellison* [1941], although the concept of *St. simulator* (in a strict sense) is restricted to the forms that are close to the species holotype [Barrick et al., 2008; Chernykh, 2005]. *St. simulator* in the Moscow Basin occurs in the upper Rusavkino Formation, while in the Donets Basin this species has been found in the O<sub>6</sub> limestone [Goreva and Alekseev, 2007].

[23] The Carboniferous-Permian boundary (base of the Asselian Stage) in the exposed Donets Basin resides within the Kartamyshskaya Formation. In the subsurface Predonets Trough the first Asselian fusulinids are found at the correlative analog of the Q<sub>7</sub> “grey zone” of the exposed Donets Basin [Davydov et al., 1992]. Palynological [Inosova et al., 1976] and paleomagnetic data [Davydov, 1986] also suggest the position of the Carboniferous-Permian boundary at the Q<sub>7</sub> “grey zone.”

#### 4. U-Pb Geochronology

[24] At least 37 volcanic ash beds (among them 25 coal tonsteins) have been reported in the Donets Basin [Chernov'yants, 1992]. Tonstein (German for “clay stone”) is a widely used term for a volcanic ash bed within a coal seam; tonsteins are widely used for correlation in the coal basins of eastern and western Europe [Burger et al., 1997]. Tonsteins have been reported from Donets Basin coals since extensive coal production in the 19th century, and possess the local term “seriki” (meaning grayish rock within the coal), but their volcanic origin was recognized much later when they were used for correlation of specific coals within the basin [Zaritskiy, 1977]. The oldest tonsteins are reported from the Samarskaya [C<sub>1</sub> (C)] Formation in the subsurface of the western

Donets Basin [Savchuk, 1957], while the youngest tonsteins are reported from the N<sub>2</sub> limestone. We collected 40 volcanic ash samples from sections, localities, and shafts, but only 12 produced datable zircon crystal populations. These samples range from the C<sub>1b</sub><sup>upper</sup> to the C<sub>3a</sub> (n<sub>1</sub> coal) biostratigraphic zones. Four samples came from surface localities and eight samples are tonsteins collected from productive coals in commercial shafts (Table 1 and Figure 1). All samples collected from surface localities are completely altered to bentonite.

#### 4.1. Methods

[25] Zircon was subjected to a modified version of the chemical abrasion method of Mattinson [2005], reflecting a preference to prepare and analyze carefully selected single crystals. Zircon separates were placed in a muffle furnace at 900°C for 60 h in quartz beakers. Single annealed grains were selected and transferred to 3 ml Teflon PFA beakers with ultrapure H<sub>2</sub>O and then loaded into 300 μl Teflon PFA microcapsules. Fifteen microcapsules were placed in a large-capacity Parr vessel, and the crystals partially dissolved in 120 μl of 29 M HF for 10–12 h at 180°C. The contents of each microcapsule were returned to 3 ml Teflon PFA beakers, the HF removed and the residual grains rinsed in ultrapure H<sub>2</sub>O, immersed in 3.5 M HNO<sub>3</sub>, ultrasonically cleaned for an hour, and fluxed on a hotplate at 80°C for an hour. The HNO<sub>3</sub> was removed and the grains were rinsed several times with ultrapure H<sub>2</sub>O before being reloaded into the same 300 μl Teflon PFA microcapsules (themselves rinsed and fluxed in 6 M HCl during crystal sonication and washing) and spiked with the EARTHTIME mixed <sup>205</sup>Pb-<sup>233</sup>U-<sup>235</sup>U tracer solution (ET535). The grains were dissolved in Parr vessels in 120 μl of 29 M HF with a trace of 3.5 M HNO<sub>3</sub> at 220°C for 48 h, dried to salts, and then redissolved in 6 M HCl in Parr vessels at 180°C overnight. U and Pb were separated from the zircon matrix using an HCl-based anion exchange chromatographic procedure [Krogh, 1973], eluted together and dried with 2 μl of 0.05 N H<sub>3</sub>PO<sub>4</sub>.

[26] Pb and U were loaded on a single outgassed Re filament in 2 μl of a silica gel/phosphoric acid mixture [Gerstenberger and Haase, 1997], and U and Pb isotopic measurements made on a GV Isoprobe-T multicollector thermal ionization mass spectrometer equipped with an ion-counting Daly detector. Pb isotopes were measured by peak jumping all isotopes on the Daly detector for 100 to 150 cycles, and corrected for 0.22 ± 0.04%/

**Table 1.** Summary of Volcanic Ash Samples and Ages

| Sample Name | Sample Type | Thickness (cm) | Location   | Latitude (°N) | Longitude (°E) | Lithostratigraphic Index | Biostratigraphic Zone   | $^{206}\text{Pb}/^{238}\text{U}$ Age (Ma) | MSWD | Probability of Fit | n        |
|-------------|-------------|----------------|--|---------------|----------------|--------------------------|-------------------------|---|------|--------------------|----------|
| n1 coal     | tonstein    | 17–20          | Butovskaya Shaft   | 48.0677       | 37.7918        | n <sub>1-lower</sub>     | base C <sub>3a</sub>    | 307.26 ± 0.11                             | 3.8  | 0.000              | 9 of 12  |
| m3 coal     | tonstein    | 15–20          | Zasyadko Shaft   | 48.0517       | 37.7939        | m <sub>3</sub>           | middle C <sub>2c</sub>  | 310.55 ± 0.10                             | 2.2  | 0.018              | 10 of 11 |
| l3(a) coal  | tonstein    | 3–5            | Krasnolimanskaya Shaft                                     | 48.3594       | 37.2430        | l <sub>3</sub>           | middle C <sub>2b</sub>  | 312.01 ± 0.08                             | 1.4  | 0.220              | 6 of 7   |
| l3(b) coal  | tonstein    | 1–2            | Zdanovskaya Shaft  | 48.1309       | 38.2699        | l <sub>3</sub> (?)       | middle C <sub>2b</sub>  | 312.18 ± 0.07                             | 0.2  | 0.980              | 6 of 10  |
| l1 coal     | tonstein    | 3–5            | Kirov Shaft  | 48.1320       | 38.3548        | l <sub>1</sub>           | base C <sub>2b</sub>    | 312.23 ± 0.09                             | 1.7  | 0.140              | 5 of 11  |
| k7 coal     | tonstein    | 3–5            | Pereval'skaya Shaft  | 48.4460       | 38.80          | k <sub>7</sub>           | upper C <sub>2a</sub>   | 313.16 ± 0.08                             | 0.6  | 0.800              | 8 of 8   |
| k3 coal     | tonstein    | 1–2            | Pereval'skaya Shaft  | 48.4460       | 38.80          | k <sub>3</sub>           | base of C <sub>2a</sub> | 314.40 ± 0.06                             | 1.5  | 0.180              | 7 of 9   |
| c11 coal    | tonstein    | 2–3            | Yuzhno-Donbasskaya Shaft No 3, Ugleclad                    | 47.7839       | 37.2474        | c <sub>11</sub>          | middle C <sub>1g2</sub> | 328.14 ± 0.11                             | 2.6  | 0.012              | 8 of 10  |
| C1ve2       | bentonite   | 1–2            | Sukhaya Volnovakha, Dokuchaevsk, Tsentral'nyi rudnik, east | 47.73         | 37.6503        | C <sub>1A9</sub>         | base C <sub>1e2</sub>   | 342.01 ± 0.10                             | 1.9  | 0.073              | 7 of 8   |
| C1vc        | bentonite   | 5–8            | Sukhaya Volnovakha, Dokuchaevsk, Tsentral'nyi rudnik, east | 47.72         | 37.6502        | C <sub>1A8</sub>         | upper C <sub>1c</sub>   | 345.00 ± 0.08                             | 0.9  | 0.460              | 6 of 7   |
| 3/2002      | bentonite   | 10–15          | Sukhaya Volnovakha, Dokuchaevsk, Tsentral'nyi rudnik, east | 47.73         | 37.6503        | C <sub>1A8</sub>         | middle C <sub>1c</sub>  | 345.17 ± 0.07                             | 1.2  | 0.320              | 6 of 8   |
| 5/2002      | bentonite   | 15–20          | Volnovakha River right bank, near Businova Ravine          | 47.6398       | 37.8926        | C <sub>1A4</sub>         | base C <sub>1b2</sub>   | 357.26 ± 0.08                             | 0.7  | 0.660              | 8 of 8   |

a.m.u. (atomic mass unit) mass fractionation. Transitory isobaric interferences due to high-molecular weight organics, particularly on  $^{204}\text{Pb}$  and  $^{207}\text{Pb}$ , disappeared within approximately 30 cycles, while ionization efficiency averaged  $10^4$  cps/pg of each Pb isotope. Linearity (to  $\geq 1.4 \times 10^6$  cps) and the associated dead time correction of the Daly detector were monitored by repeated analyses of NBS982, and have been constant since installation. Uranium was analyzed as  $\text{UO}_2^+$  ions in static Faraday mode on  $10^{11}$  ohm resistors for 150 to 200 cycles, and corrected for isobaric interference of  $^{233}\text{U}^{18}\text{O}^{16}\text{O}$  on  $^{235}\text{U}^{16}\text{O}^{16}\text{O}$  with an  $^{18}\text{O}/^{16}\text{O}$  of 0.00205. Ionization efficiency averaged 20 mV/ng of each U isotope. U mass fractionation was corrected using the known  $^{233}\text{U}/^{235}\text{U}$  ratio of the ET535 tracer solution.

[27] U-Pb dates and uncertainties were calculated using the algorithms of *Schmitz and Schoene* [2007],  $^{235}\text{U}/^{205}\text{Pb} = 100.206$  and  $^{233}\text{U}/^{235}\text{U} = 0.9946$  for the ET535 spike [*Condon et al.*, 2007], and the U decay constants of *Jaffey et al.* [1971].  $^{206}\text{Pb}/^{238}\text{U}$  ratios and dates were corrected for initial  $^{230}\text{Th}$  disequilibrium using a  $\text{Th}/\text{U}_{[\text{magma}]}$  of 3, resulting in a systematic increase in the  $^{206}\text{Pb}/^{238}\text{U}$  dates of  $\sim 90$  kyr. All common Pb in analyses was attributed to laboratory blank and subtracted based on the measured laboratory Pb isotopic composition and associated uncertainty. U blanks were  $< 0.1$  pg, and small compared to sample amounts. Over the course of the experiment, isotopic analyses of the TEMORA zircon standard [*Black et al.*, 2003] yielded a weighted mean  $^{206}\text{Pb}/^{238}\text{U}$  age of  $417.43 \pm 0.06$  (n = 11, MSWD = 0.8; Figure 3).

## 4.2. Results

[28] Concordant U-Pb dates were obtained from 106 of 110 analyzed zircon grains from the 12 dated samples (Table 2 and Figure 4). Ages of the samples (Table 1) are interpreted from the weighted means of the  $^{206}\text{Pb}/^{238}\text{U}$  dates, based on 5–10 grains per sample that are equivalent in age, calculated using Isoplot 3.0 [*Ludwig*, 2003]. Grains that are older than those used in the calculations (n = 8) are interpreted as inherited antecrysts, and grains that are younger (n = 12) are thought to have suffered severe Pb loss not completely mitigated by chemical abrasion. Errors on individual analyses are based upon nonsystematic analytical uncertainties, including counting statistics, spike subtraction, and blank Pb subtraction. Similarly nonsystematic errors on weighted mean dates are reported as internal  $2\sigma$  for

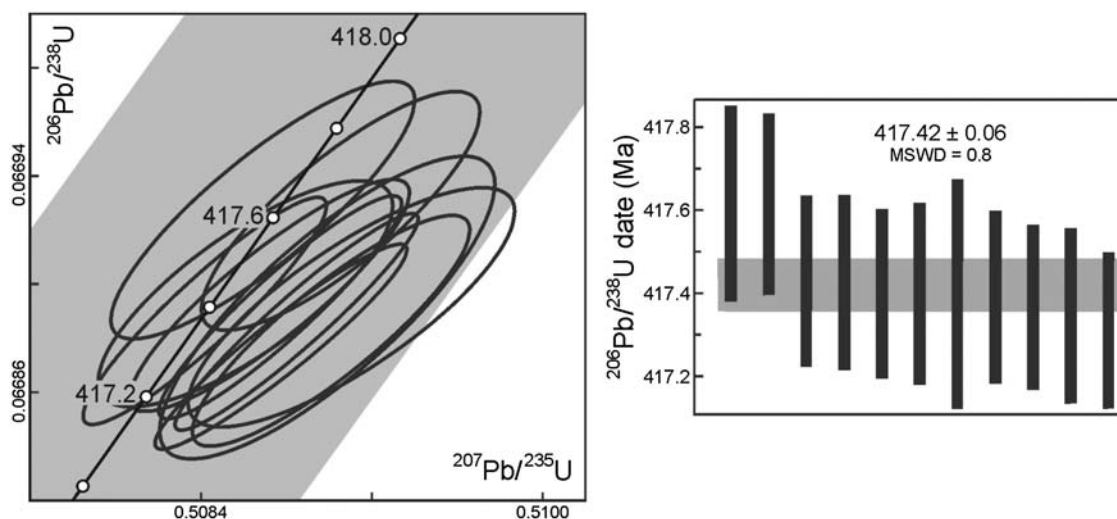


**Figure 3.** Concordia diagram and ranked  $^{206}\text{Pb}/^{238}\text{U}$  age plot for chemically abraded zircon single grain analyses of the TEMORA natural zircon standard.

the nine samples with probability of fit of  $>0.05$  on the weighted mean date. For the three samples with probability of fit  $<0.05$ , errors are at the 95% confidence interval, which is the internal  $2\sigma$  error expanded by the square root of the MSWD and the Student's T multiplier of  $n - 1$  degrees of freedom. These error estimates should be considered when comparing our  $^{206}\text{Pb}/^{238}\text{U}$  dates with those from other laboratories that used the same EARTHTIME spike or a spike that was cross calibrated using EARTHTIME gravimetric standards. When comparing our dates with those derived from other decay schemes (e.g.,  $^{40}\text{Ar}/^{39}\text{Ar}$ ,  $^{187}\text{Re}-^{187}\text{Os}$ ), the uncertainties in the tracer calibration and  $^{238}\text{U}$  decay constant should be added to the internal error in quadrature. This total error ranges from  $\pm 0.36$  Myr for the youngest sample to  $\pm 0.42$  Myr for the oldest sample.

[29] Eight analyzed grains from sample 5-2002 yielded a weighted mean  $^{206}\text{Pb}/^{238}\text{U}$  date of  $357.26 \pm 0.08$  Ma (MSWD = 0.7). Six of the eight analyzed grains from sample 3-2002 yielded a weighted mean date of  $345.17 \pm 0.07$  Ma (MSWD = 1.2). Two other grains are younger. Six of the seven analyzed grains from sample C1vc yielded a weighted mean date of  $345.00 \pm 0.08$  Ma (MSWD = 0.9). One other grain is younger. Seven of the eight analyzed grains from sample C1ve2 yielded a weighted mean date of  $342.01 \pm 0.10$  Ma (MSWD = 1.9). One other grain is younger. Eight of the 10 analyzed grains from sample c11 coal yielded a weighted mean date of  $328.14 \pm 0.11$  Ma (MSWD = 2.6). Two other grains are slightly younger.

[30] Seven of the nine analyzed grains from sample k3 coal yielded a weighted mean  $^{206}\text{Pb}/^{238}\text{U}$  date of  $314.40 \pm 0.06$  Ma (MSWD = 1.5). Two other grains are older. Eight analyzed grains from sample k7 coal yielded a weighted mean date of  $313.16 \pm 0.08$  Ma (MSWD = 0.6). Five of the 11 analyzed grains from sample l<sub>1</sub> coal yielded a weighted mean date of  $312.23 \pm 0.09$  Ma (MSWD = 1.7). One other grain is older and five others are younger. Six of the 10 analyzed grains from sample l3(b) coal yielded a weighted mean date of  $312.18 \pm 0.07$  Ma (MSWD = 0.2). Four other grains are older. Six of the seven analyzed grains from sample l3(a) coal yielded a weighted mean date of  $312.01 \pm 0.08$  Ma (MSWD = 1.4). One other grain is slightly older. Ten of the 11 analyzed grains from sample m3 coal yielded a weighted mean date of  $310.55 \pm 0.10$  Ma (MSWD = 2.2). One other grain is older. Nine of the 12 analyzed grains from sample n1 coal yielded a weighted mean date of  $307.26 \pm 0.11$  Ma (MSWD = 3.8). Three other grains are slightly younger.

## 5. Discussion

### 5.1. Frequency Patterns of Cyclothem Sedimentation

[31] Since *Wanless and Shepard* [1936] first proposed that cyclothem sedimentary packages in the midcontinent of North America resulted from marine transgressions and regressions across the shelf driven by glacioeustatic fluctuations, numerous studies have argued the merits of Milankovitch

**Table 2 (Sample).** U-Pb Isotopic Data [The full Table 2 is available in the HTML version of this article]

| Grain <sup>a</sup> | Th/U <sup>b</sup> | <sup>206</sup> Pb* <sup>c</sup><br>(× 10 <sup>-13</sup> mol) | mol %<br><sup>206</sup> Pb* <sup>c</sup> | Pb*/<br>Pbc <sup>c</sup> | Pbc <sup>c</sup><br>(pg) | Radiogenic Isotopic Ratios                           |  |  |                         |   |                         |   |                         |
|--------------------|-------------------|--|--|--------------------------|--------------------------|--|--|--|-------------------------|---|-------------------------|---|-------------------------|
|                    |                   |  |  |                          |                          | <sup>206</sup> Pb/<br><sup>204</sup> Pb <sup>d</sup> | <sup>208</sup> Pb/<br><sup>206</sup> Pb <sup>e</sup> | <sup>207</sup> Pb/<br><sup>206</sup> Pb <sup>e</sup> | %<br>Error <sup>f</sup> | <sup>207</sup> Pb/<br><sup>235</sup> U <sup>e</sup> | %<br>Error <sup>f</sup> | <sup>206</sup> Pb/<br><sup>238</sup> U <sup>e</sup> | %<br>Error <sup>f</sup> |
| <i>n1 Coal</i>     |                   |  |  |                          |                          |  |  |  |                         |   |                         |   |                         |
| <b>z1</b>          | <b>0.445</b>      | <b>2.3123</b>  | <b>99.69%</b>                            | <b>96</b>                | <b>0.60</b>              | <b>5958</b>  | <b>0.141</b>   | <b>0.052547</b>                                      | <b>0.104</b>            | <b>0.353379</b>                                     | <b>0.135</b>            | <b>0.048775</b>                                     | <b>0.051</b>            |
| z2                 | 0.421             | 2.7308   | 99.71%                                   | 101                      | 0.66                     | 6307   | 0.133  | 0.052577   | 0.089                   | 0.353304  | 0.121                   | 0.048737  | 0.047                   |
| z3                 | 0.467             | 2.3059   | 99.68%                                   | 95                       | 0.60                     | 5857   | 0.148  | 0.052581   | 0.093                   | 0.352847  | 0.125                   | 0.048669  | 0.048                   |
| <b>z4</b>          | <b>0.423</b>      | <b>2.7728</b>  | <b>99.78%</b>                            | <b>133</b>               | <b>0.51</b>              | <b>8361</b>  | <b>0.134</b>   | <b>0.052504</b>                                      | <b>0.076</b>            | <b>0.353500</b>                                     | <b>0.111</b>            | <b>0.048831</b>                                     | <b>0.050</b>            |
| z5                 | 0.419             | 2.2417   | 99.66%                                   | 88                       | 0.62                     | 5548   | 0.132  | 0.052529   | 0.106                   | 0.352781  | 0.137                   | 0.048709  | 0.050                   |
| <b>z6</b>          | <b>0.393</b>      | <b>2.2391</b>  | <b>99.68%</b>                            | <b>92</b>                | <b>0.59</b>              | <b>5822</b>  | <b>0.124</b>   | <b>0.052499</b>                                      | <b>0.098</b>            | <b>0.353375</b>                                     | <b>0.130</b>            | <b>0.048818</b>                                     | <b>0.051</b>            |
| <b>z7</b>          | <b>0.421</b>      | <b>2.9845</b>  | <b>99.79%</b>                            | <b>139</b>               | <b>0.52</b>              | <b>8735</b>  | <b>0.133</b>   | <b>0.052486</b>                                      | <b>0.077</b>            | <b>0.353059</b>                                     | <b>0.112</b>            | <b>0.048787</b>                                     | <b>0.050</b>            |
| <b>z8</b>          | <b>0.443</b>      | <b>1.4164</b>  | <b>99.35%</b>                            | <b>46</b>                | <b>0.76</b>              | <b>2878</b>  | <b>0.140</b>   | <b>0.052456</b>                                      | <b>0.176</b>            | <b>0.352997</b>                                     | <b>0.204</b>            | <b>0.048806</b>                                     | <b>0.053</b>            |
| <b>z9</b>          | <b>0.417</b>      | <b>2.5827</b>  | <b>99.63%</b>                            | <b>80</b>                | <b>0.79</b>              | <b>5016</b>  | <b>0.132</b>   | <b>0.052464</b>                                      | <b>0.108</b>            | <b>0.353149</b>                                     | <b>0.139</b>            | <b>0.048819</b>                                     | <b>0.049</b>            |
| <b>z10</b>         | <b>0.508</b>      | <b>1.5607</b>  | <b>99.55%</b>                            | <b>67</b>                | <b>0.58</b>              | <b>4114</b>  | <b>0.161</b>   | <b>0.052452</b>                                      | <b>0.138</b>            | <b>0.353200</b>                                     | <b>0.166</b>            | <b>0.048838</b>                                     | <b>0.052</b>            |
| <b>z11</b>         | <b>0.449</b>      | <b>2.2164</b>  | <b>99.72%</b>                            | <b>108</b>               | <b>0.50</b>              | <b>6747</b>  | <b>0.142</b>   | <b>0.052527</b>                                      | <b>0.084</b>            | <b>0.353728</b>                                     | <b>0.117</b>            | <b>0.048841</b>                                     | <b>0.048</b>            |
| <b>z12</b>         | <b>0.388</b>      | <b>2.1318</b>  | <b>99.49%</b>                            | <b>57</b>                | <b>0.90</b>              | <b>3623</b>  | <b>0.122</b>   | <b>0.052460</b>                                      | <b>0.177</b>            | <b>0.353289</b>                                     | <b>0.200</b>            | <b>0.048843</b>                                     | <b>0.056</b>            |
| <i>m3 Coal</i>     |                   |  |  |                          |                          |  |  |  |                         |   |                         |   |                         |
| <b>z1</b>          | <b>0.473</b>      | <b>1.2310</b>  | <b>99.39%</b>                            | <b>49</b>                | <b>0.62</b>              | <b>3054</b>  | <b>0.149</b>   | <b>0.052528</b>                                      | <b>0.169</b>            | <b>0.357563</b>                                     | <b>0.198</b>            | <b>0.049369</b>                                     | <b>0.054</b>            |
| <b>z2</b>          | <b>0.772</b>      | <b>0.9099</b>  | <b>99.49%</b>                            | <b>63</b>                | <b>0.39</b>              | <b>3632</b>  | <b>0.244</b>   | <b>0.052638</b>                                      | <b>0.163</b>            | <b>0.357944</b>                                     | <b>0.194</b>            | <b>0.049319</b>                                     | <b>0.061</b>            |
| <b>z3</b>          | <b>0.569</b>      | <b>0.8638</b>  | <b>99.34%</b>                            | <b>47</b>                | <b>0.47</b>              | <b>2839</b>  | <b>0.180</b>   | <b>0.052466</b>                                      | <b>0.198</b>            | <b>0.357176</b>                                     | <b>0.232</b>            | <b>0.049374</b>                                     | <b>0.071</b>            |
| <b>z4</b>          | <b>0.597</b>      | <b>1.7040</b>  | <b>99.21%</b>                            | <b>39</b>                | <b>1.12</b>              | <b>2349</b>  | <b>0.189</b>   | <b>0.052576</b>                                      | <b>0.419</b>            | <b>0.357974</b>                                     | <b>0.429</b>            | <b>0.049381</b>                                     | <b>0.098</b>            |
| <b>z5</b>          | <b>0.723</b>      | <b>1.3036</b>  | <b>99.25%</b>                            | <b>43</b>                | <b>0.81</b>              | <b>2488</b>  | <b>0.229</b>   | <b>0.052623</b>                                      | <b>0.200</b>            | <b>0.357835</b>                                     | <b>0.235</b>            | <b>0.049318</b>                                     | <b>0.073</b>            |
| <b>z7</b>          | <b>0.530</b>      | <b>1.5848</b>  | <b>99.50%</b>                            | <b>61</b>                | <b>0.65</b>              | <b>3730</b>  | <b>0.167</b>   | <b>0.052530</b>                                      | <b>0.206</b>            | <b>0.357368</b>                                     | <b>0.226</b>            | <b>0.049341</b>                                     | <b>0.065</b>            |
| <b>z8</b>          | <b>0.575</b>      | <b>0.8294</b>  | <b>99.40%</b>                            | <b>51</b>                | <b>0.41</b>              | <b>3086</b>  | <b>0.182</b>   | <b>0.052698</b>                                      | <b>0.140</b>            | <b>0.358780</b>                                     | <b>0.184</b>            | <b>0.049378</b>                                     | <b>0.065</b>            |
| z10                | 0.670             | 0.4357   | 98.53%                                   | 21                       | 0.53                     | 1266   | 0.211  | 0.053151   | 0.409                   | 0.392705  | 0.455                   | 0.053586  | 0.123                   |
| <b>z11</b>         | <b>0.475</b>      | <b>0.7702</b>  | <b>98.97%</b>                            | <b>29</b>                | <b>0.66</b>              | <b>1807</b>  | <b>0.150</b>   | <b>0.052611</b>                                      | <b>0.286</b>            | <b>0.357850</b>                                     | <b>0.322</b>            | <b>0.049332</b>                                     | <b>0.070</b>            |
| <b>z12</b>         | <b>0.518</b>      | <b>1.7218</b>  | <b>99.42%</b>                            | <b>53</b>                | <b>0.82</b>              | <b>3232</b>  | <b>0.164</b>   | <b>0.052628</b>                                      | <b>0.159</b>            | <b>0.358079</b>                                     | <b>0.188</b>            | <b>0.049347</b>                                     | <b>0.055</b>            |
| <b>z13</b>         | <b>0.448</b>      | <b>1.7148</b>  | <b>99.32%</b>                            | <b>43</b>                | <b>0.97</b>              | <b>2719</b>  | <b>0.141</b>   | <b>0.052493</b>                                      | <b>0.188</b>            | <b>0.357360</b>                                     | <b>0.218</b>            | <b>0.049374</b>                                     | <b>0.058</b>            |
| <i>l3(a) Coal</i>  |                   |  |  |                          |                          |  |  |  |                         |   |                         |   |                         |
| <b>z1</b>          | <b>0.816</b>      | <b>0.9797</b>  | <b>99.62%</b>                            | <b>87</b>                | <b>0.30</b>              | <b>4950</b>  | <b>0.258</b>   | <b>0.052710</b>                                      | <b>0.120</b>            | <b>0.360422</b>                                     | <b>0.160</b>            | <b>0.049593</b>                                     | <b>0.075</b>            |
| <b>z2</b>          | <b>0.779</b>      | <b>1.2037</b>  | <b>99.59%</b>                            | <b>79</b>                | <b>0.41</b>              | <b>4506</b>  | <b>0.246</b>   | <b>0.052592</b>                                      | <b>0.124</b>            | <b>0.359520</b>                                     | <b>0.158</b>            | <b>0.049579</b>                                     | <b>0.061</b>            |
| <b>z4</b>          | <b>0.598</b>      | <b>3.2498</b>  | <b>99.74%</b>                            | <b>121</b>               | <b>0.69</b>              | <b>7260</b>  | <b>0.189</b>   | <b>0.052625</b>                                      | <b>0.066</b>            | <b>0.360016</b>                                     | <b>0.107</b>            | <b>0.049617</b>                                     | <b>0.051</b>            |
| z5                 | 0.615             | 2.0242   | 99.61%                                   | 80                       | 0.65                     | 4766   | 0.194  | 0.052556   | 0.114                   | 0.360614  | 0.145                   | 0.049765  | 0.054                   |
| <b>z8</b>          | <b>0.709</b>      | <b>0.8590</b>  | <b>98.89%</b>                            | <b>29</b>                | <b>0.79</b>              | <b>1681</b>  | <b>0.224</b>   | <b>0.052515</b>                                      | <b>0.277</b>            | <b>0.358981</b>                                     | <b>0.312</b>            | <b>0.049578</b>                                     | <b>0.059</b>            |
| <b>z9</b>          | <b>1.031</b>      | <b>0.7023</b>  | <b>98.72%</b>                            | <b>27</b>                | <b>0.75</b>              | <b>1454</b>  | <b>0.327</b>   | <b>0.052752</b>                                      | <b>0.373</b>            | <b>0.360783</b>                                     | <b>0.406</b>            | <b>0.049602</b>                                     | <b>0.084</b>            |
| <b>z11</b>         | <b>0.757</b>      | <b>2.3855</b>  | <b>99.64%</b>                            | <b>90</b>                | <b>0.71</b>              | <b>5182</b>  | <b>0.239</b>   | <b>0.052658</b>                                      | <b>0.107</b>            | <b>0.359942</b>                                     | <b>0.142</b>            | <b>0.049575</b>                                     | <b>0.061</b>            |
| <i>l3(b) Coal</i>  |                   |  |  |                          |                          |  |  |  |                         |   |                         |   |                         |
| <b>z1</b>          | <b>0.594</b>      | <b>2.7913</b>  | <b>99.73%</b>                            | <b>113</b>               | <b>0.63</b>              | <b>6787</b>  | <b>0.188</b>   | <b>0.052611</b>                                      | <b>0.094</b>            | <b>0.359870</b>                                     | <b>0.125</b>            | <b>0.049610</b>                                     | <b>0.049</b>            |
| z3                 | 0.354             | 1.1140   | 99.44%                                   | 52                       | 0.51                     | 3338   | 0.113  | 0.053424   | 0.161                   | 0.375059  | 0.189                   | 0.050917  | 0.048                   |
| <b>z4</b>          | <b>0.580</b>      | <b>2.8870</b>  | <b>99.78%</b>                            | <b>139</b>               | <b>0.53</b>              | <b>8359</b>  | <b>0.183</b>   | <b>0.052623</b>                                      | <b>0.124</b>            | <b>0.360000</b>                                     | <b>0.147</b>            | <b>0.049616</b>                                     | <b>0.054</b>            |
| <b>z5</b>          | <b>0.744</b>      | <b>2.1387</b>  | <b>99.73%</b>                            | <b>118</b>               | <b>0.48</b>              | <b>6811</b>  | <b>0.235</b>   | <b>0.052532</b>                                      | <b>0.082</b>            | <b>0.359394</b>                                     | <b>0.120</b>            | <b>0.049619</b>                                     | <b>0.056</b>            |
| z6                 | 0.799             | 0.7426   | 98.92%                                   | 30                       | 0.66                     | 1730   | 0.252  | 0.052676   | 0.299                   | 0.366532  | 0.339                   | 0.050466  | 0.092                   |
| <b>z7</b>          | <b>0.500</b>      | <b>1.7489</b>  | <b>99.65%</b>                            | <b>86</b>                | <b>0.51</b>              | <b>5263</b>  | <b>0.158</b>   | <b>0.052689</b>                                      | <b>0.150</b>            | <b>0.360494</b>                                     | <b>0.172</b>            | <b>0.049622</b>                                     | <b>0.057</b>            |
| <b>z8</b>          | <b>1.135</b>      | <b>1.1406</b>  | <b>99.48%</b>                            | <b>67</b>                | <b>0.49</b>              | <b>3552</b>  | <b>0.359</b>   | <b>0.052686</b>                                      | <b>0.145</b>            | <b>0.360458</b>                                     | <b>0.179</b>            | <b>0.049621</b>                                     | <b>0.064</b>            |
| <b>z9</b>          | <b>1.093</b>      | <b>1.5625</b>  | <b>99.54%</b>                            | <b>75</b>                | <b>0.60</b>              | <b>4015</b>  | <b>0.345</b>   | <b>0.052590</b>                                      | <b>0.135</b>            | <b>0.359823</b>                                     | <b>0.165</b>            | <b>0.049623</b>                                     | <b>0.053</b>            |
| z11                | 0.439             | 1.4138   | 99.56%                                   | 68                       | 0.51                     | 4239   | 0.139  | 0.052670   | 0.123                   | 0.362944  | 0.155                   | 0.049977  | 0.054                   |
| z12                | 0.877             | 0.9080   | 99.12%                                   | 37                       | 0.66                     | 2107   | 0.277  | 0.052663   | 0.331                   | 0.360838  | 0.352                   | 0.049694  | 0.082                   |

<sup>a</sup> Labels z1, z2, etc., are for analyses composed of single zircon grains or fragments. Labels in bold denote analyses used in the weighted mean date calculations. Zircon was annealed and chemically abraded [Mattinson, 2005].

<sup>b</sup> Model Th/U ratio calculated from radiogenic <sup>208</sup>Pb/<sup>206</sup>Pb ratio and <sup>207</sup>Pb/<sup>235</sup>U date.

<sup>c</sup> Pb\* and Pbc are radiogenic and common Pb, respectively; mol % <sup>206</sup>Pb\* is with respect to radiogenic and blank Pb.

<sup>d</sup> Measured ratio corrected for spike and fractionation only. Fractionation correction is 0.22 ± 0.02 (1-sigma) %/amu (atomic mass unit) for single-collector Daly analyses, based on analysis of NBS-981 and NBS-982.

<sup>e</sup> Corrected for fractionation, spike, common Pb, and initial disequilibrium in <sup>230</sup>Th/<sup>238</sup>U. Common Pb is assigned to procedural blank with composition of <sup>206</sup>Pb/<sup>204</sup>Pb = 18.60 ± 0.80%, <sup>207</sup>Pb/<sup>204</sup>Pb = 15.69 ± 0.32%, and <sup>208</sup>Pb/<sup>204</sup>Pb = 38.51 ± 0.74% (1-sigma); <sup>206</sup>Pb/<sup>238</sup>U and <sup>207</sup>Pb/<sup>206</sup>Pb ratios corrected for initial disequilibrium in <sup>230</sup>Th/<sup>238</sup>U using Th/U [magma] = 3.

<sup>f</sup> Errors are 2-sigma, propagated using algorithms of Schmitz and Schoene [2007].

<sup>g</sup> Calculations based on the decay constants of Jaffey et al. [1971]; <sup>206</sup>Pb/<sup>238</sup>U and <sup>207</sup>Pb/<sup>206</sup>Pb dates corrected for initial disequilibrium in <sup>230</sup>Th/<sup>238</sup>U using Th/U [magma] = 3.

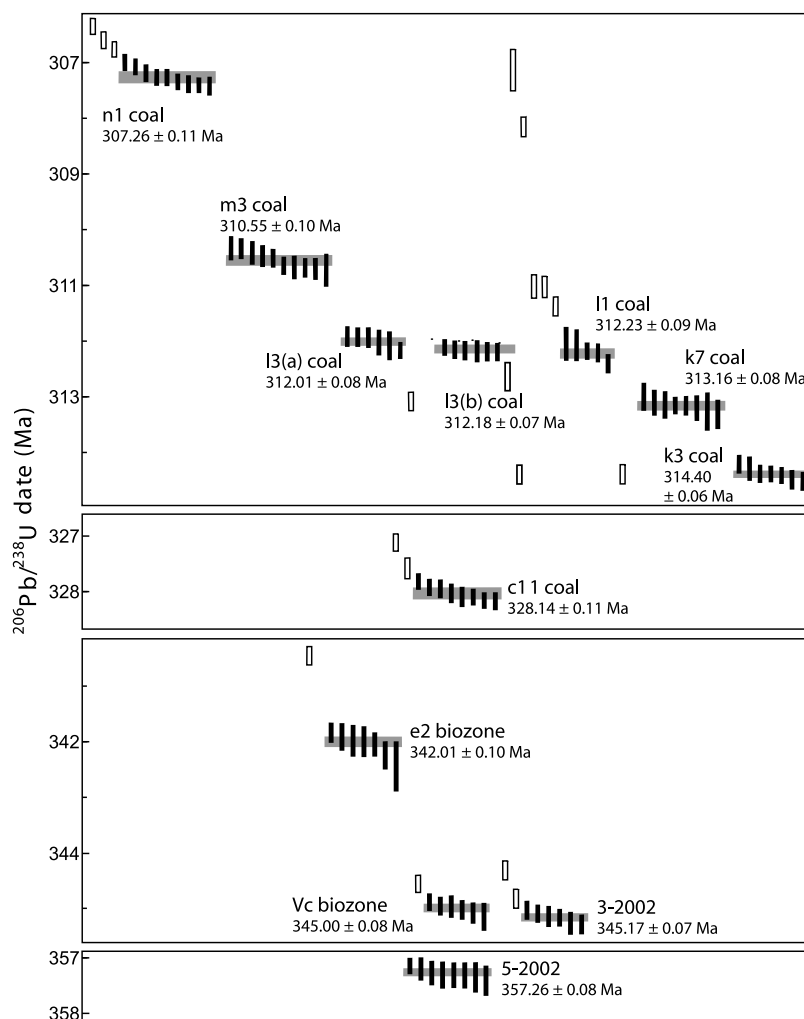


**Figure 4.** Ranked  $^{206}\text{Pb}/^{238}\text{U}$  age plots for all single zircon analyses from Donets Basin tuffs.

orbital modulation of cyclic sedimentary deposition in the late Paleozoic [Algeo and Wilkinson, 1988; Boardman and Heckel, 1989; Dickinson et al., 1994; Heckel, 1986; Klein and Willard, 1989; Klein, 1990; Soreghan and Dickinson, 1994; Soreghan and Giles, 1999]. A demonstration of Milankovitch band orbital forcing in the late Paleozoic record not only has significant implications for our understanding the growth and demise of the Gondwanan ice sheet and modeling of concomitant climate change [Birgenheier et al., 2009; Montanez et al., 2007; Poulsen et al., 2007], but also holds considerable promise as a high-resolution chronometric ruler for calibrating and testing global biostratigraphic and sequence stratigraphic correlations [Haq and Schutter, 2008; Heckel et al., 2007; Ross and Ross, 1988].

[32] Unfortunately, due to a paucity of radiometric age constraints for the Carboniferous, early arguments for and against orbitally driven sedimentary

cyclicality relied upon a priori assumptions of the duration or rate of sedimentation combined with cycle counting in a given stratigraphic sequence [Algeo and Wilkinson, 1988]. As the assumed durations of various regional stages of the Carboniferous have substantively changed [Hess and Lippolt, 1986; Hess et al., 1999], so the robustness of estimated cycle frequencies has been compromised [Heckel, 1986, 1994; Klein, 1990]. More recently, application of U-Pb geochronology to pedogenic carbonates [Rasbury et al., 1998] has provided direct dating within Pennsylvanian to Early Permian cyclic sediments of New Mexico and west Texas. The resulting cycle period estimate of  $143 \pm 64$  ka for these North American cyclothem was among the first to highlight likely short-period eccentricity forcing of late Paleozoic sedimentary cycles, similar to glacioeustatic cycles of the Pleistocene. Nonetheless, this estimate required correlation of relatively low precision ( $\pm 2-3$  Ma)

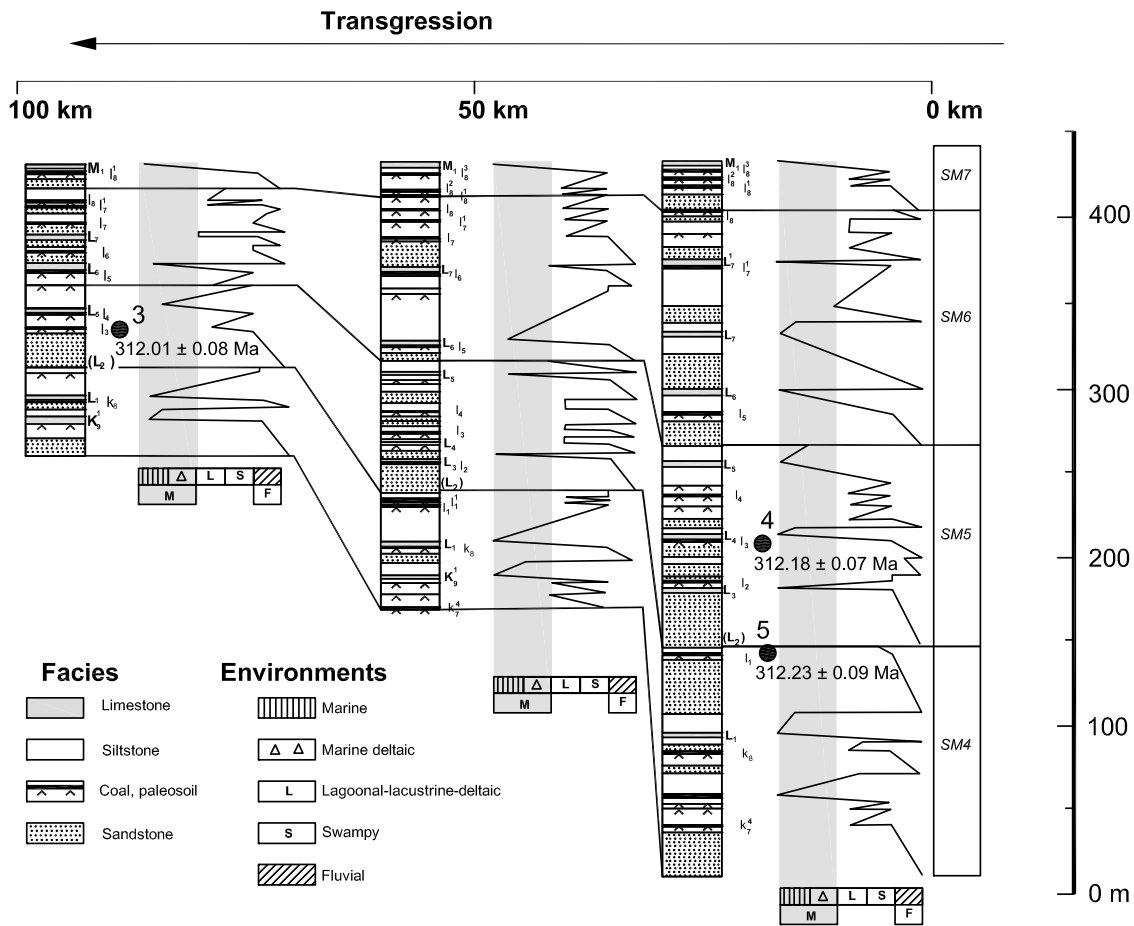


**Figure 5.** East-west transgressive-regressive cycles and stratal correlations in the  $C_2^6$  (L) Almaznaya Formation with position of dated samples (after *Izart et al.* [1996], copyright 1996, with permission from Elsevier). The transgressive nature of the coals is obvious, as are minor unconformities at sequence boundaries; nonetheless, radiometric dating demonstrates that proposed correlations across the basin are robust at a resolution of  $\sim 100$  ka.

ages between two different basins, and counting of cycles in sections from the Sacramento Mountains that have [*Rasbury et al.*, 1998, p. 404] “. . . more of a nonmarine influence and are less likely to be complete.”

[33] Innovations in ID-TIMS U-Pb zircon analysis [*Condon et al.*, 2007; *Mattinson*, 2005; *Mundil et al.*, 2004; *Schmitz and Schoene*, 2007] have lead to the acquisition of precise and accurate ages for Permo-Carboniferous volcanic ash beds with resolution ( $\pm \sim 100$  ka) within the Milankovitch band. *Gastaldo et al.* [2009] report two ID-TIMS U-Pb zircon ages for Serpukhovian tonsteins within the Upper Silesian Basin of eastern Europe. A tonstein in the Ludmila coal ( $328.84 \pm 0.16$  Ma) within the middle Petřkovice Member of the Ostrava Formation in the Upper Silesian Basin, and a tonstein in the Karel coal of the Hrušov Member ( $328.01 \pm 0.08$  Ma) are separated by eleven clearly defined marine transgressive-regressive cycles analogous

to (although apparently older than) the classical Pennsylvanian cyclothems of the Appalachian basin. The resulting cycle duration estimate of  $83 \pm 24$  ka overlaps at the 95% confidence interval with the short-period ( $\sim 100$  ka) eccentricity cycle among potential orbital forcing mechanisms. These results from widely different basins and different Carboniferous stages provide significant support for orbital eccentricity forcing of climate in the late Paleozoic Ice Age. Our new radiometric ages in the Donets Basin similarly allow for the direct dating and calculation of the periodicity of Pennsylvanian cycles.

[34] In order to calibrate the cyclicity of the Donets Basin, we draw upon the work of *Izart et al.* [1996, 2002, 2003, 2006] who interpreted the Serpukhovian through Gzhelian successions of the Donets Basin in terms of sequence stratigraphy, and proposed a hierarchy of high-frequency, fourth-, third- and second-order sequences. Figures 5–7 repro-

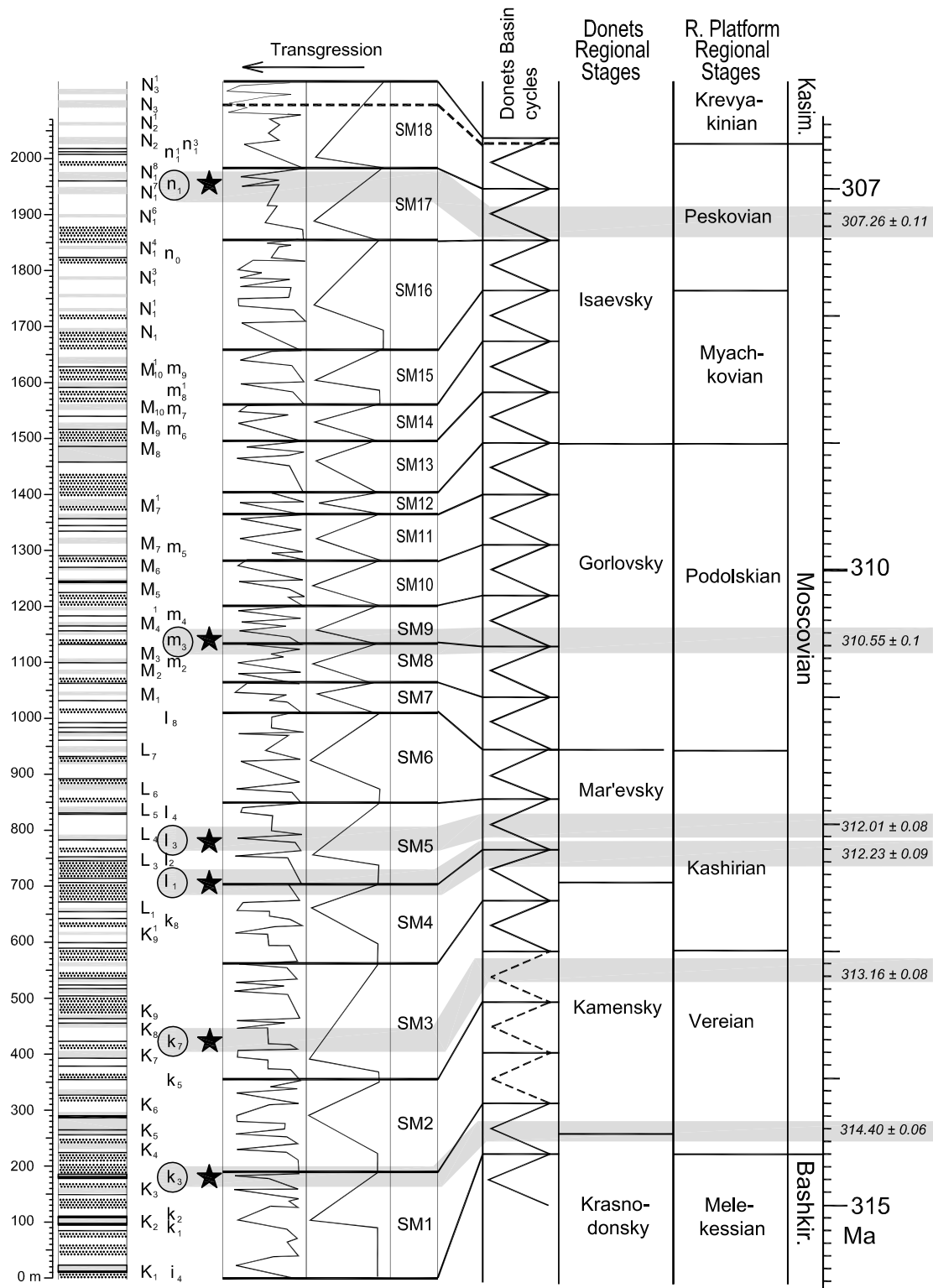


**Figure 6.** Lithostratigraphy and sequence stratigraphy through the Moscovian succession of the central exposed Donets Basin (modified from *Izart et al.* [1996, Figure 3]), with positions of six radiometric ages obtained in our study. Projection of stratigraphic architecture onto a time linear scale constrained by ash bed ages reveals the consistent  $\sim 400$  ka tempo of the fourth-order sequences of *Izart et al.* [1996]. Only a few high-frequency cycles in the lowermost Moscovian must be reinterpreted as fourth-order major transgressions to maintain consistency with the model. Tuning of these fourth-order sequences to the long eccentricity cycle allows calibration of the biostratigraphic record at a resolution of  $\sim 100$  ka.

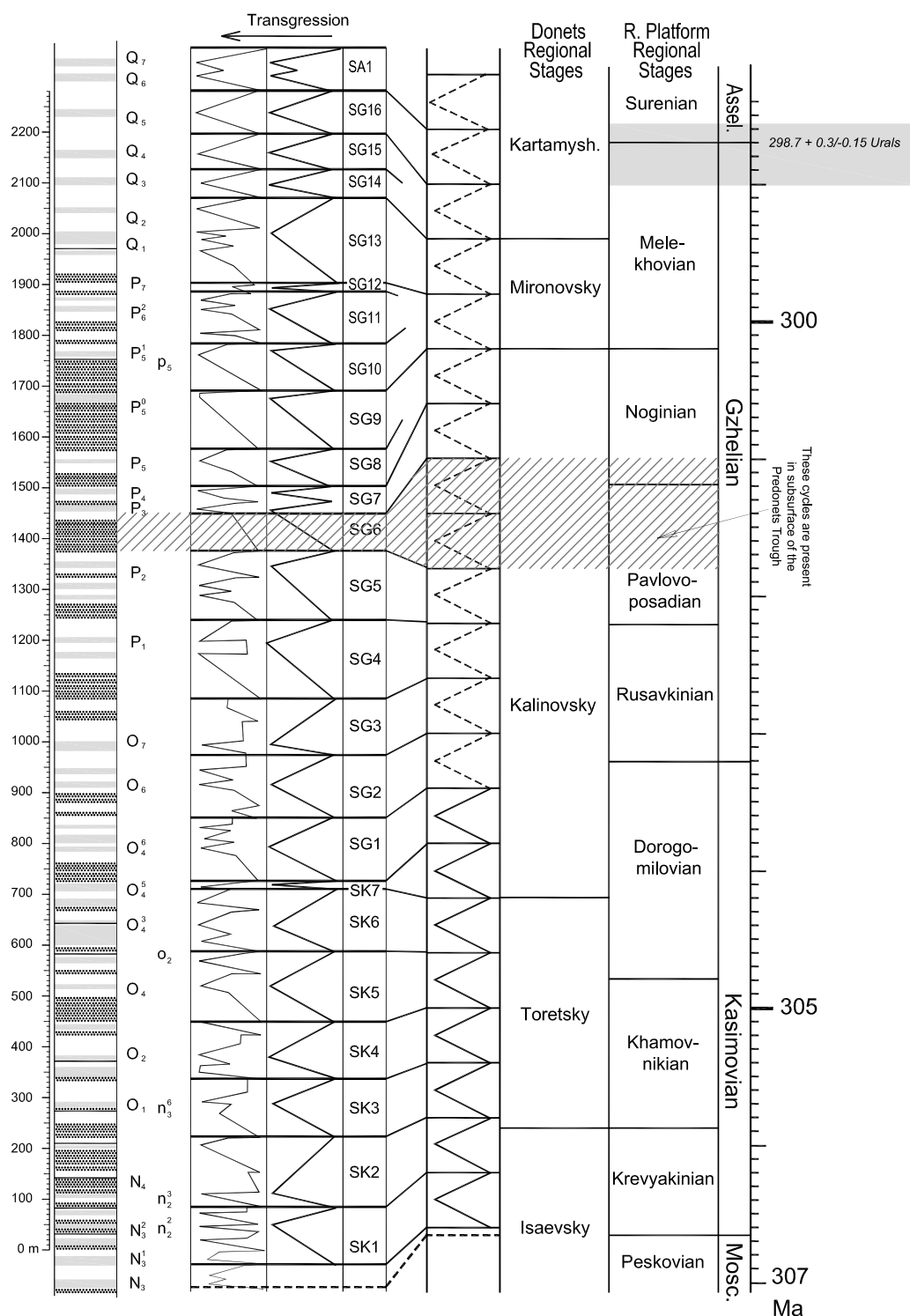


**Figure 7.** Lithostratigraphy and sequence stratigraphy through the Kasimovian-Gzhelian succession of the central exposed Donets Basin (modified from *Izart et al.* [2006, Figure 12]). The long eccentricity cycle tuning of fourth-order sequences derived for the Moscovian succession is extrapolated upward to the Carboniferous-Permian boundary constrained at 298.7 Ma [*Ramezani et al.*, 2007] in the Usolka parastratotype section of the Urals. High-frequency and fourth-order sequences of the Kasimovian and early Gzhelian are well developed, lending more confidence to the cyclostratigraphic calibration. Although cyclicality becomes more ambiguous in the increasingly continental upper Gzhelian succession, only modest reinterpretation of *Izart et al.*'s [2006] fourth-order sequences as higher-frequency cycles is necessary to align the base of the Asselian in the Donets Basin with the radiometric constraint from the Urals.





duce aspects of their compiled lithostratigraphic logs and interpreted transgressive-regressive cycles of the Donets Basin, annotated with the stratigraphic position and age of our dated tonsteins projected onto a linear time axis. *Izart et al.* [1996] divided the Moscovian succession into eighteen fourth-order sequences defined by bundles of one major and several minor marine transgressions recorded as limestone bands with or without underlying coals (for example, Figure 5). Five ash bed ages from the  $k_3$  through  $n_1$  coals span a total of sixteen fourth-order sequences; ashes are separated by <1, 2, 4, 6, 8 and 16 cycles. For each pair of radiometric ages, regardless of position, the calculated cycle duration is  $\sim 400$  ka (ten total constraints). We interpret this reproducible cycle duration as robust evidence for long-period eccentricity forcing via glacioeustasy of the major marine transgressions defining these fourth-order sequences. Perhaps the most remarkable demonstration of the resolving power of our improved radiometric methods comes from the 200 ka age difference between the  $l_1$  and  $l_3$  coals, by which we are able to parse time within the long-period eccentricity cycle. This resolution has important implications as it strongly suggests that at least some of the high-frequency sequences of *Izart et al.* [1996] record short-period ( $\sim 100$  ka) eccentricity cycle forcing, which are in turn modulated to give the fourth-order major transgressive cycles at the  $\sim 400$  ka beat frequency. A corollary to this conclusion is that the amount of time contained in a single cyclothem transgressive-regressive sedimentary packet is  $\sim 100$  ka or less, as has been previously suggested by *Rasbury et al.* [1998].

[35] We have tuned the Moscovian fourth-order sequences to the long eccentricity cycle in order to provide a high-resolution ( $\sim 100$  ka) calibration of the biostratigraphic record of the Donets Basin (Figure 6), and by aforementioned correlation the zonations of the Russian Platform and western Europe. Only a few high-frequency cycles in the lowermost Moscovian must be reinterpreted as fourth-order major transgressions to maintain consistency with the model. In this way new absolute age constraints on the base and duration of the Moscovian and its constituent regional substages and biozones have been derived (Figure 2). The implications of these new age constraints are described in section 5.2 on global time scale calibration.

[36] In Figure 7, the long eccentricity cycle tuning of fourth-order sequences derived for the Mosco-

vian succession is extrapolated upward to the Carboniferous-Permian boundary, which is constrained at 298.7 Ma [*Ramezani et al.*, 2007] in the Usolka auxiliary parastratotype section of the Urals. High-frequency and fourth-order sequences of the Kasimovian and early Gzhelian are well developed, lending confidence to our extrapolated cyclostratigraphic calibration. In this way the bases and durations of the Kasimovian and Gzhelian Stages are derived. Although the order of cyclic sequences becomes more ambiguous in the increasingly continental upper Gzhelian succession, only modest reinterpretation of *Izart et al.*'s [2006] fourth-order sequences as higher-frequency cycles is necessary to align the base of the Asselian in the Donets Basin with the radiometric constraint from the Urals. These minor modifications have been made taking into account lithostratigraphic, biostratigraphic and magnetostratigraphic characteristics of the more complete marine Gzhelian succession studied in boreholes of the eastern Pre-Donets Trough. The implication of this agreement in radiometric (Urals) and paleomagnetic (Donets) versus tuned cyclostratigraphic (Donets) model fits to the base of the Asselian is that the first appearance of the conodont index *Streptognathodus isolatus* is truly synchronous at the  $\sim 100$  ka resolution of the age model. The remarkable fidelity of the fourth-order sequences in the Donets Basin and their tuning to the 400 ka long eccentricity cycle provide a powerful chronostratigraphic tool, which we use below to provide absolute age constraints on the global time scale.

## 5.2. Application of New Ages to the Global Time Scale

[37] The new radiometric ages obtained in our study require significant revisions to the absolute age calibration of the global Carboniferous time scale. Our new ages meet the necessary prerequisites for global time scale calibration: all radiometric samples were collected and documented within the well-established local lithostratigraphic framework of the Donets Basin [*Aisenverg et al.*, 1963, 1975], and the collected samples are therefore precisely constrained within the exceptionally complete biostratigraphic framework of the basin [*Aisenverg et al.*, 1979; *Davydov*, 1992; *Davydov et al.*, 2008; *Fohrer et al.*, 2007; *Nemyrovska et al.*, 1999; *Poletaev et al.*, 1991]. As we have emphasized in our description of the Donets Basin succession, its multitaxa biostratigraphy may be straightforwardly correlated with the Tournaisian and Viséan type sections in western Europe, and



the Serpukhovian, Bashkirian, Moscovian, Kasimovian, Gzhelian and Asselian type sections in the Moscow Basin and Urals (Figure 2).

[38] Our new age constraints from the lower Mokrovolnovakhskaya [ $C_1^1$  (A)] Series go some way toward remedying the dearth of radiometric (and particularly ID-TIMS U-Pb zircon) ages for the global Mississippian subperiod [Davydov *et al.*, 2004; Menning *et al.*, 2006]. The age of  $357.26 \pm 0.08$  Ma obtained from an ash near the base of the  $C_1^1b_2$  biostratigraphic zone is consistent with an age for the Devonian-Carboniferous boundary of 359.2 Ma, and supports the proposition of a much shorter duration of the Hastarian Substage of the Tournaisian in western Europe [Davydov *et al.*, 2004; Haq and Schutter, 2008; Menning *et al.*, 2006]. Two samples collected within and at the top of the  $C_1^1c$  zone—which reliably correlates with the lower Moliniacian (Late Chadian) of the lowermost Viséan in western Europe—provide a minimum age of 346.3 Ma for the base of the global Viséan Stage, i.e., one million years older than proposed in the most recent global time scale compilations [Davydov *et al.*, 2004; Menning *et al.*, 2006]. An age of  $342.01 \pm 0.10$  Ma from a bentonite in the lower Styl'skaya Formation extends the duration of the Tulian and consequently the Holkerian Substage up to 6 Ma.

[39] A very dramatic change in the global time scale is provided by the new age of  $328.14 \pm 0.11$  Ma obtained from the  $c_{11}$  coal sample, in the  $C_1^1g_2$  biozone. According to foraminifera (*Betpakodiscus cornuspiroides*) and ammonoids (*Eumorphoceras*) this coal correlates with the lower Steshevian Horizon of the Serpukhovian in the Russian Platform, and the Pendleian (*Eumorphoceras* 1 Zone) of western Europe. This age pushes the lower boundary of the Serpukhovian down to approximately 330 Ma, i.e., about 4 Ma older than in previous global time scale compilations. Similar ages were recently obtained from the aforementioned tonsteins in the Upper Silesian Basin [Gastaldo *et al.*, 2009]. Their host strata correlate with the lower and middle Pendleian Substage of western Europe, thus the age estimate of 330 Ma for the base of Serpukhovian proposed here is in excellent agreement with the extrapolated age of 329.7 Ma suggested from the Silesian Basin.

[40] Prior radiometric calibrations of the Pennsylvanian time scale relied mainly upon a series of  $^{40}\text{Ar}/^{39}\text{Ar}$  sanidine ages from the Donets Basin [Hess *et al.*, 1999], the Upper Silesian Basin and several central European (Sahr, Ruhr, Bohemian,

IntraSudetic) basins [Burger *et al.*, 1997; Hess and Lippolt, 1986]. Our radiometric date for the  $l_3$  coal of the Donets basin of  $312.01 \pm 0.08$  Ma may be directly compared to the result of Hess *et al.* [1999] for the  $l_3$  coal of  $305.5 \pm 1.5$  Ma. Beyond the obvious contrast in precision, the accuracy of the significantly younger  $^{40}\text{Ar}/^{39}\text{Ar}$  sanidine age is clearly called into question. Even taking into account systematic errors associated with decay constants and monitor standards [Kuiper *et al.*, 2008; Min *et al.*, 2000; Renne *et al.*, 1998; Villeneuve *et al.*, 2000] this sanidine age is anomalously young. Although this phenomenon was noted and interpreted as indicating systematic problems with biostratigraphic correlation [Hess *et al.*, 1999], it is apparent from our results that instead this age suffers from a systematic analytical or geological bias. The fidelity of  $^{40}\text{Ar}/^{39}\text{Ar}$  sanidine ages from other European basins is similarly suspect, although the large errors on these ages make it generally difficult to assess the degree of bias [Davydov *et al.*, 2004]. In summary, these imprecise Carboniferous sanidine ages appear to be plagued by one or a combination of systematic analytical errors and open system behavior, and are thus superseded by our new accurate and precise U-Pb ages for Pennsylvanian time scale calibration.

[41] Our most extensive dating of tonsteins has been from the Moscovian Stage, as many shafts are actively mining coal of this age. Seven ages were obtained from coals  $k_3$ ,  $k_7$ ,  $l_1$ ,  $l_3$  (two samples from different shafts),  $m_3$ , and  $n_1$  (Tables 1 and 2). These samples and their associated cyclostratigraphic calibration of the Late Pennsylvanian dramatically change our understanding of the distribution of time in the Moscovian Stage. The base of the stage shifts down to 314.6 Ma (one fourth-order cycle below coal  $k_3$  from which the oldest Moscovian age was obtained). The top of the Moscovian (e.g., the base of the traditional Kasimovian in the  $N_3$  limestone) is calibrated as 306.7 Ma, thus the duration of the Moscovian Stage increases up to 7.9 Ma as oppose to 6–7 Ma in most recent global time scale compilations [Davydov *et al.*, 2004; Menning *et al.*, 2006].

[42] We note that both the traditional and alternative definitions for the base of the Kasimovian Stage can be assigned numerical ages based upon our tuned cyclostratigraphic model for the Late Pennsylvanian. The traditional base of the Kasimovian (at the FADs of fusilinid *Protriticites pseudomontiparus* and the conodont *Streptognathodus subexcelsus*) in the  $N_3$  limestone is calibrated as 306.7 Ma. On the



other hand the FAD of the conodont *Idiognathodus sagittalis* in the O<sub>1</sub> limestone is calibrated at 305.6 Ma. In the latter case the durations of the Moscovian and Kasimovian Stages change to 9.0 and 2.4 Ma, respectively.

[43] The base of the Gzhelian Stage, taken as the FAD of the conodont *Streptognathodus simulator*, is calibrated via the extension of our tuned cyclostratigraphic model at 303.2 Ma, thus constraining the durations of the traditional Kasimovian (3.5 Ma) and the Gzhelian Stages (4.5 Ma). This age of the base of the Gzhelian Stage in the Donets Basin is in good agreement with independent geochronological data for the same FAD in the Usolka section of the southern Urals [Schmitz *et al.*, 2005]. Similarly, although cyclicity becomes more ambiguous in the increasingly continental upper Gzhelian succession, only modest reinterpretation of Izart *et al.*'s [2006] fourth-order sequences as higher-frequency cycles is necessary to align the base of the Asselian in the Donets Basin with the radiometric constraint of 298.7 Ma from the Urals [Ramezani *et al.*, 2007].

## 6. Conclusions

[44] We have provided a robust demonstration via high-precision U-Pb CA-TIMS zircon geochronology that the classical Pennsylvanian cyclothem preserved in the Donets Basin are the record of Milankovitch orbital eccentricity forcing of sea level. Given the established similarities in sedimentology and stratal architectures between cyclothem of the Donets Basin and those of the midcontinent United States [Heckel, 2002; Heckel *et al.*, 2007] we tentatively extend this model to the latter, in support of prior inferences of eccentricity forcing [Chesnut, 1996; Heckel, 1994, 2002, 2008]. Variation in glacioeustatic response is inherent to short- versus long-period eccentricity cycle modulation, and is consistent with the three existing radiometric cycle period calibrations in diachronous and globally distributed basins [Gastaldo *et al.*, 2009; Rasbury *et al.*, 1998]. Further biostratigraphic correlation studies and radiometric dating will provide additional tests of this model extension to other cyclic sedimentary succession of the Carboniferous and Early Permian [Barrick *et al.*, 2004; Heckel *et al.*, 2007; Ritter, 1995]. A reexamination of the Donets Basin cyclostratigraphy using more detailed sedimentological criteria and quantitative frequency domain analysis is also necessary to refine and identify the Milankovitch parameters

responsible for the higher-frequency cycles of the basin.

[45] The radiometrically calibrated cyclostratigraphy of the Donets Basin provides a Pennsylvanian chronostratigraphic framework of unprecedented resolution (~100 ka), which directly constrains numerous regional biostratigraphic zonations and the global time scale. In addition, new ages in the Mississippian succession of the Donets Basin also significantly change our understanding of the distribution of time in the global scale, with implications for the correlation of emerging near- and far-field records of climate change during the early stages of the late Paleozoic Ice Age.

## Acknowledgments

[46] The authors acknowledge financial support from National Science Foundation grants EAR-MRI 0521221, EAR-SGP 0418703, and EAR-SGP 0545247. Field work was aided by Isabel Montanez, Mike Eros, and Tamara Nemirovskaya. We thank Director of Donetskgeologia Zhikalyak Nikolai Vasilievich and Chief Geologist Bondar'Aleksandr Pavlovich for providing access to information and data.

## References

- Aisenverg, D. E., et al. (1963), *Carboniferous Stratigraphy of the Donets Basin*, 183 pp., Publ. House of Ukrainian Acad. of Sci., Kiev.
- Aisenverg, D. E., et al. (1971), *Atlas of Fauna of Carboniferous Deposits of Donets Basin*, 327 pp., Nauk. Dumka, Kiev.
- Aisenverg, D. E., et al. (1975), Field excursion guide book for the Donets Basin (in Russian), in *Compte Rendu of the 8th International Congress on Carboniferous Stratigraphy and Geology*, pp. 1–360, edited by D. E. Aisenverg et al., Nauka, Moscow.
- Aizenverg, D. E., et al. (1979), Pervyye nakhodki goniatitov v otlozheniyakh svit C<sub>1</sub>A i C<sub>1</sub>C Donetskogo basseyna (The first goniatite findings in the C<sub>1</sub>A and C<sub>1</sub>C suites of the Donets Basin), *Geol. Zh.*, 39(6), 32–40.
- Aizenverg, D. E., et al. (1983), *Verkhneserpukhovskiy Pod'yarus Donetskogo Basseyna (Paleontologicheskaya Kharakteristika)*, 163 pp., Akad. Nauk Ukrainskoy SSR, Inst. Geol. Nauk, Nauk. Dumka, Kiev.
- Alekseev, A. S., and N. V. Goreva (2006), Kasimovian and Gzhelian (Upper Pennsylvanian) conodont zonation in Russia, *Newsl. Carboniferous Stratigr.*, 24, 40–43.
- Algeo, T. J., and B. H. Wilkinson (1988), Periodicity of mesoscale Phanerozoic sedimentary cycles and the role of Milankovitch orbital modulation, *J. Geol.*, 96(3), 313–322, doi:10.1086/629222.
- Barrick, J. E., et al. (2004), Pennsylvanian conodont zonation for midcontinent North America, *Rev. Esp. Micropaleontol.*, 36, 231–250.
- Barrick, J. E., et al. (2008), Revision of the conodont *Idiognathodus simulator* (Ellison 1941), the marker species for the base of the Late Pennsylvanian global Gzhelian Stage, *Micropaleontology*, 54, 125–137.
- Barskov, I. S., and A. S. Alekseyev (1975), Konodonty srednego i verkhnego karbona Podmoskov'ya (Conodonts of the middle



- and upper Carboniferous from the vicinity of Moscow), *Izv. Akad. Nauk SSSR, Ser. Geol.*, 6, 84–99.
- Belka, Z., and J. Lehmann (1998), Late Visean/early Namurian conodont succession from the Esla area of the Cantabrian Mountains, Spain, *Acta Geol. Pol.*, 48(1), 31–41.
- Birgenheier, L. P., et al. (2009), Evidence for dynamic climate change on sub-106-year scales from the late Paleozoic glacial record, Tamworth Belt, New South Wales, Australia, *J. Sediment. Res.*, 79, 56–82, doi:10.2110/jsr.2009.013.
- Black, L., et al. (2003), TEMORA 1: A new zircon standard for Phanerozoic U–Pb geochronology, *Chem. Geol.*, 200(1–2), 155–170, doi:10.1016/S0009-2541(03)00165-7.
- Boardman, D. R. II, and P. H. Heckel (1989), Glacial-eustatic sea-level curve for early Late Pennsylvanian sequence in north-central Texas and biostratigraphic correlation with curve for midcontinent North America, *Geology*, 17(9), 802–805, doi:10.1130/0091-7613(1989)017<0802:GESLFC>2.3.CO;2.
- Brazhnikova, N. E., et al. (1967), *Mikrofaunisticheskiye markiruyushchiye gorizonty kamennougol'nykh i permskikh otlozheniy Dneprovsko-Donetskoy vpadiny (Microfaunal Marker Horizons in the Carboniferous and Permian Deposits of the Dnieper-Donets Basin)*, 285 pp., Akad. Nauk Ukr. SSR, Inst. Geol. Nauk, Kiev.
- Briand, C., et al. (1998), Stratigraphy and sequence stratigraphy of the Moscovian, Kasimovian and Gzhelian in the Moscow Basin, *Bull. Soc. Geol. Fr.*, 169(1), 35–52.
- Burger, K., et al. (1997), Tephrochronologie mit Kaolin-Kohlentonsteinen: Mittel zur Korrelation paralischer und limnischer Ablagerungen des Oberkarbons, *Geol. Jahrb., Reihe A*, 147, 3–39.
- Chekunov, A. V. (1994), The geodynamics of the Dniepr-Donets rift syncline (in Russian), *Geophysics*, 16(3), 3–13.
- Chernov'yants, M. G. (1992), *Tonshteyni i ikh ispol'zovanie pri izuchenii ugljosnykh formatsiy (Tonsteins and Their Utilization in Coal-Bearing Deposits Study)*, 130 pp., Nedra, Moscow.
- Chernykh, V. V. (2002), Zonal scale of the Gzhelian and Kasimovian stages based on conodonts of genus *Streptognathodus* (in Russian), in *Stratigraphy and Paleogeography of Carboniferous of Eurasia*, edited by B. I. Chuvashov and E. A. Amon, pp. 302–306, Inst. of Geol. and Geochem., Uralian Branch, Russ. Acad. of Sci., Ekaterinburg.
- Chernykh, V. V. (2005), Zonal Method in Biostratigraphy: Zonal Conodont Scale of the Lower Permian in the Urals (in Russian), 217 pp., Inst. of Geol. and Geochemistry, Uralian Branch, Russ. Acad. of Sci., Ekaterinburg.
- Chernykh, V. V., and N. P. Reshetkova (1987), The Biostratigraphy and Conodonts From Carboniferous-Permian Boundary Deposits on the West Slope of the Central and Southern Urals (in Russian), 53 pp., Uralian Branch, USSR Acad. of Sci., Sverdlovsk.
- Chernykh, V. V., B. I. Chuvashov, V. I. Davydov, M. D. Schmitz, and W. S. Snyder (2006), Usolka section (southern Urals, Russia): A potential candidate for GSSP to define the base of the Gzhelian Stage in the global chronostratigraphic scale, *Geologija*, 49(2), 205–217.
- Chesnut, D. R. (1996), Geologic framework for the coal-bearing rocks of the Central Appalachian Basin, *Int. J. Coal Geol.*, 31, 55–66.
- Condon, D., et al. (2007), EARTHTIME: Isotopic tracers and optimized solutions for high-precision U–Pb ID-TIMS geochronology, *Eos Trans. AGU*, 88(52), Fall Meet. Suppl., Abstract V41E–06.
- Cozar, P., et al. (2008), Late Visean-Serpukhovian foraminiferans and calcareous algae from the Adarouch region (central Morocco), North Africa, *Geol. J.*, 43(4), 463–485, doi:10.1002/gj.1119.
- Davydov, V. I. (1986), Precise definition of the Carboniferous-Permian boundary in Donets Basin and the northern Caucasus based on paleomagnetic criteria, *Sov. Geol.*, no. 12, 74–76.
- Davydov, V. I. (1990), Zonal fusulinid subdivisions of Gzhelian in Donets Basin and Pre-Donets Trough, in *Problems of Modern Micropaleontology*, pp. 52–69, Nauka, Saint Petersburg, Russia.
- Davydov, V. I. (1992), Subdivision and correlation of Upper Carboniferous and Lower Permian deposits in Donets Basin according to fusulinid data (in Russian), *Sov. Geol.*, no. 5, 53–61.
- Davydov, V. I. (1997), Middle/Upper Carboniferous boundary: The problem of definition and correlation, in *Proceeding of the XIII International Congress on the Carboniferous and Permian*, edited by M. Podemski et al., pp. 113–122, Pol. Geol. Inst., Warsaw.
- Davydov, V. I. (2009), Bashkirian-Moscovian transition in Donets Basin: The key for Tethyan-Boreal correlation, in *The Carboniferous Type Sections in Russia, Potential and Proposed Stratotypes: Proceedings of the International Conference*, pp. 188–192, Inst. of Geol., Bashkirian Acad. of Sci., Ufa, Russia.
- Davydov, V. I., and R. Khodjanyazova (2009), Moscovian-Kasimovian transition in Donets Basin: Fusulinid taxonomy, biostratigraphy correlation and paleobiogeography, in *The Carboniferous Type Sections in Russia, Potential and Proposed Stratotypes: Proceedings of the International Conference*, pp. 193–196, Inst. of Geol., Bashkirian Acad. of Sci., Ufa, Russia.
- Davydov, V. I., and A. V. Popov (1991), The Carboniferous system (in Russian), in *Zonal Stratigraphy of the Phanerozoic of the U.S.S.R.*, pp. 64–76, Nedra, Moscow.
- Davydov, V. I., et al. (1992), The Carboniferous-Permian boundary in the former USSR and its correlation, *Int. Geol. Rev.*, 34(9), 889–906, doi:10.1080/00206819209465643.
- Davydov, V. I., et al. (2004), The Carboniferous period, in *A Geologic Time Scale 2004*, edited by F. M. Gradstein et al., pp. 222–248, Cambridge Univ. Press, Cambridge, U. K.
- Davydov, V. I., et al. (2008), Faunal assemblage and correlation of Kasimovian-Gzhelian transition at Usolka section, southern Urals, Russia (a potential candidate for GSSP to define base of Gzhelian Stage), *Stratigraphy*, 5(2), 113–135.
- Devuyt, F.-X., and J. Kalvoda (2007), Early evolution of the genus *Eoparastaffella* (Foraminifera) in Eurasia; the “intericta group” and related forms, late Tournaisian to early Visean (Mississippian), *J. Foraminiferal Res.*, 37(1), 69–89, doi:10.2113/gsjfr.37.1.69.
- Devuyt, F.-X., et al. (2003), A proposed global stratotype section and point for the base of the Visean Stage (Carboniferous): The Pengchong Section, Guangzi, south China, *Epi-sodes*, 26(2), 105–115.
- Dickinson, W. R., et al. (1994), Glacio-eustatic origin of Permo-Carboniferous stratigraphic cycles; evidence from the southern Cordilleran foreland region, in *Concepts in Sedimentology and Paleontology*, vol. 4, edited by J. M. Dennison and F. R. Ettensohn, pp. 25–34, Soc. for Sediment. Geol., Tulsa, Okla.
- Ellison, S. P., Jr. (1941), Revisions of Pennsylvanian conodonts, *J. Paleontol.*, 15, 107–143.
- Fisunenko, O. P. (2000), *On the Problem of the Moscovian Stage*, 115 pp., Lugansk Pedagogical Inst., Lugansk, Ukraine.
- Fohrer, B., et al. (2007), The Pennsylvanian (Moscovian) Izvarino section, Donets Basin, Ukraine: A multidisciplinary study on microfacies, biostratigraphy (conodonts, forami-



- fers, and ostracodes), and paleoecology, *J. Paleontol.*, 81(5), 1–85.
- Gastaldo, R. A., et al. (2009), Ecological persistence in the Late Mississippian (Serpukhovian–Namurian A) megafloral record of the Upper Silesian Basin, Czech Republic, *Palaios*, 24(6), 336–350, doi:10.2110/palo.2008.p08-084r.
- Gavrish, V. K. (Ed.) (1989), *Geology and Oil and Gas Potential of the Dniepr-Donets Depression, Depth Structure and Geotectonic Evolution* (in Russian), 208 pp., Nauk. Dumka, Kiev.
- Gerstenberger, H., and G. Haase (1997), A highly effective emitter substance for mass spectrometric Pb isotope ratio determinations, *Chem. Geol.*, 136, 309–312, doi:10.1016/S0009-2541(96)00033-2.
- Goreva, N. V., and A. S. Alekseev (2007), Correlation of upper Carboniferous (Pennsylvanian) deposits in the Moscow Syncline and Donets Basin by conodonts, in *Paleontological Investigations in Ukraine: History, Current Status and Perspectives*, edited by P.F. Gozhik et al., pp. 110–114, Nauk. Dumka, Kiev.
- Grozdilova, L. P. (1966), Foraminifery verkhnego karbona severnogo Timana (Foraminifera of the upper Carboniferous of the northern Timan range), in *Trudy Vsesoyuznogo Neftyanogo Nauchno-Issledovatel'skogo Geologorazvedochnogo Instituta*, pp. 254–331, Nedra, Leningrad.
- Haq, B. U., and S. R. Schutter (2008), A chronology of Paleozoic sea-level changes, *Science*, 322(5898), 64–68, doi:10.1126/science.1161648.
- Heckel, P. H. (1986), Sea-level curve for Pennsylvanian eustatic marine transgressive-regressive depositional cycles along midcontinent outcrop belt, North America, *Geology*, 14(4), 330–334, doi:10.1130/0091-7613(1986)14<330:SCFPEM>2.0.CO;2.
- Heckel, P. H. (1994), Evaluation of evidence for glacio-eustatic control over marine Pennsylvanian cyclothem in North America and consideration of possible tectonic events, in *Concepts in Sedimentology and Paleontology*, edited by J. M. Dennison and F. R. Etnessohn, pp. 65–87, Soc. for Sediment. Geol., Tulsa, Okla.
- Heckel, P. H. (2002), Overview of Pennsylvanian cyclothem in midcontinent North America and brief summary of those elsewhere in the world, *Can. Soc. Pet. Geol. Mem.*, 19, 79–98.
- Heckel, P. H. (2008), Pennsylvanian cyclothem in midcontinent North America as far-field effects of waxing and waning of Gondwana ice sheets, *Spec. Pap. Geol. Soc. Am.*, 441, 275–289.
- Heckel, P. H., et al. (2007), Cyclothem [“digital”] correlation and biostratigraphy across the global Moscovian–Kasimovian–Gzhelian stage boundary interval (Middle–Upper Pennsylvanian) in North America and eastern Europe, *Geology*, 35(7), 607–610, doi:10.1130/G23564A.1.
- Heckel, P. H., et al. (2008), Choice of conodont *Idiognathodus simulator* (sensu stricto) as the event marker for the base of the global Gzhelian stage (Upper Pennsylvanian series, Carboniferous system), *Episodes*, 31(3), 319–325.
- Hess, J. C., and H. J. Lippolt (1986), <sup>40</sup>Ar/<sup>39</sup>Ar ages of tonstein and tuff sanidines: New calibration points for the improvement of the Upper Carboniferous time scale, *Chem. Geol.*, 59, 143–154.
- Hess, J. C., et al. (1999), High-precision <sup>40</sup>Ar/<sup>39</sup>Ar spectrum dating on sanidine from the Donets Basin, Ukraine: Evidence for correlation problems in the Upper Carboniferous, *J. Geol. Soc.*, 156, 527–533, doi:10.1144/gsjgs.156.3.0527.
- Inosova, K. I., et al. (1976), *Atlas of Microspores and Pollen of the Upper Carboniferous and Lower Permian of the Donets Basin*, 334 pp., Nedra, Moscow.
- Isakova, T. N., and K. Ueno (2007), About lectotype *Rauserites rossicus* (Schellwien) 1908 [Foraminifera] from the Gzhelian stage of the Donets and Moscow basins, in *Zbirnik Naukovikh Prats Institutu Geologichnikh Nauk NAN Ukraini: Biostratigraphy and Paleontology*, pp. 105–109, Nauk. Dumka, Kiev.
- Ivanova, E. A., and I. V. Khvorova (1955), *Stratigraphy of the Middle–Upper Carboniferous of the Western Part of the Moscow Syncline*, 279 pp., Russ. Acad. of Sci., Moscow.
- Izart, A., et al. (1996), Stratigraphy and sequence stratigraphy of the Moscovian in the Donets Basin, *Tectonophysics*, 268(1–4), 189–209, doi:10.1016/S0040-1951(96)00224-7.
- Izart, A., et al. (2002), Sequence stratigraphy of the Serpukhovian, Bashkirian and Moscovian in Gondwanaland, western and eastern Europe and USA, *Can. Soc. Pet. Geol. Mem.*, 19, 144–157.
- Izart, A., et al. (2003), Sequence stratigraphy and correlation of Late Carboniferous and Permian in the CIS, Europe, Tethyan area, North Africa, Arabia, China, Gondwanaland and the USA, *Palaeogeogr. Palaeoclimatol. Palaeoecol.*, 196(1–2), 59–84, doi:10.1016/S0031-0182(03)00313-4.
- Izart, A., et al. (2006), Stratigraphic distribution of macerals and biomarkers in the Donets Basin: Implications for paleoecology, paleoclimatology and eustasy, *Int. J. Coal Geol.*, 66(1–2), 69–107, doi:10.1016/j.coal.2005.07.002.
- Jaffey, A. H., et al. (1971), Precision measurement of half-lives and specific activities of <sup>235</sup>U and <sup>238</sup>U, *Phys. Rev. C*, 4, 1889–1906, doi:10.1103/PhysRevC.4.1889.
- Kabanov, P. B., et al. (2006), Biotic changes in a eustatic cyclothem: Domodedovo Formation (Moscovian, Carboniferous) of Peski quarries, Moscow region, *Paleontol. J.*, 40(4), 351–368, doi:10.1134/S0031030106040010.
- Kagarmanov, A. K., and L. M. Donakova (1990), Carboniferous system, in *Decisions of the Regional Stratigraphic Conference on the Middle and Upper Paleozoic of the Russian Platform*, edited by A. K. Kagarmanov and L. M. Donakova, pp. 1–95, Nedra, Saint Petersburg, Russia.
- Khodjanayazova, R., and V. I. Davydov (2008), Late Paleozoic foraminiferal diversity record in Donets Basin, Ukraine as a proxy of global climate dynamics, *Geol. Soc. Am. Abstr. Programs*, 40(6), 259.
- Kireeva, G. D. (1951), Stratigraficheskoe polozhenie moskovskogo yarusa v razreze Donetskogo basseyna (na osnove raspredeleniya fuzulinidy), *Byull. Mosk. Ova, Ispyt. Prir. Otd. Geol.*, 26(3), 35–51.
- Klein, G. d., and D. A. Willard (1989), Origin of the Pennsylvanian coal-bearing cyclothem of North America, *Geology*, 17(2), 152–155, doi:10.1130/0091-7613(1989)017<0152:OOTPCB>2.3.CO;2.
- Klein, G. d. (1990), Pennsylvanian time scales and cycle periods, *Geology*, 18(5), 455–457, doi:10.1130/0091-7613(1990)018<0455:PTSACP>2.3.CO;2.
- Kozitskaya, R. I., et al. (1978), *Konodonty karbona Donetskogo Basseyna (Conodonts From the Carboniferous of the Donets Basin)*, 138 pp., Nauk. Dumka, Kiev.
- Krogh, T. E. (1973), A low-contamination method for hydrothermal decomposition of zircon and extraction of U and Pb for isotopic age determinations, *Geochim. Cosmochim. Acta*, 37(3), 485–494, doi:10.1016/0016-7037(73)90213-5.
- Kuiper, K. F., et al. (2008), Synchronizing rock clocks of Earth history, *Science*, 320(5875), 500–504, doi:10.1126/science.1154339.



- Kulagina, E. I., et al. (2006), The Dombar Limestone in the south Urals and the Viséan-Serpukhovian boundary, *Newsl. Carboniferous Stratigr.*, 24, 9–11.
- Kullmann, J., et al. (2008), Goniatites et conodontes du Viséan/Serpukhovien dans les Pyrénées centrales et occidentales, France (Viséan/Serpukhovian goniatites and conodonts from the central and western Pyrenees, France), *Geobios*, 41(5), 635–656, doi:10.1016/j.geobios.2007.09.003.
- Lebedev, N. I. (1924), Materials for Donets Basin geology (in Russian), *News Ekaterinoslav Min. Inst.*, 14(2), 1–114.
- Levenshtein, M. L. (1963), Synonymic of coals and limestone in Donets Basin, in *Ugolnye basseiny i mestorozhdeniya yuga Evropeiskoi chasti SSSR (Donetskii bassein, Dneprovskii bassein, Lvovsko-Volynskii bassein, mestorozhdeniya zapadnykh oblastei Ukrainy i Moldavii, Belorussii, severnogo Kavkaza i Zakavkazya)*, edited by I. A. Kuznetsov, pp. 45–56, Gosgeolizdat, Moscow.
- Ludwig, K. R. (2003), User's manual for Isoplot 3.00, 70 pp., Berkeley Geochronol. Cent, Berkeley, Calif.
- Lutugin, L. I., and P. I. Stepanov (1913), Donets coal basin, in *Coal Minings in Russia*, pp. 112–143, Geol. Comm., Saint Petersburg, Russia.
- Makhlina, M. K., et al. (1979), Stratigraphy, biostratigraphy and paleogeography of Upper Carboniferous of the Moscow Syncline (in Russian), in *Stratigraphy, Paleontology and Paleogeography of Carboniferous of the Moscow Syncline. Transactions of Geological Foundation of Ministry of Geology of Russian Federation*, edited by M. K. Makhlina and C. M. Shik, pp. 25–69, Geol. Found. of Russ. Fed., Moscow.
- Makhlina, M. K., et al. (2001), *Sredniy karbon Moskovskoy sineklizy (yuzhnaya chast')*; v 2 tomakh, vol. 1, *Stratigrafiya (Middle Carboniferous of Southern Moscow Syncline, vol. 1, Stratigraphy)*, 244 pp., Rossiyskaya Akad. Nauk, Paleontol. Inst., Moscow.
- Mattinson, J. M. (2005), Zircon U-Pb chemical abrasion (“CA-TIMS”) method: Combined annealing and multi-step partial dissolution analysis for improved precision and accuracy of zircon ages, *Chem. Geol.*, 220, 47–66, doi:10.1016/j.chemgeo.2005.03.011.
- Menning, M., et al. (2006), Global time scale and regional stratigraphic reference scales of central and west Europe, east Europe, Tethys, south China, and North America as used in the Devonian-Carboniferous-Permian Correlation Chart 2003 (DCP 2003), *Palaeogeogr. Palaeoclimatol. Palaeoecol.*, 240(1–2), 318–372, doi:10.1016/j.palaeo.2006.03.058.
- Milanovsky, E. E. (1992), Aulacogens and aulacogeosynclines: Regularities in setting and evolution, *Tectonophysics*, 215(1–2), 55–68, doi:10.1016/0040-1951(92)90074-G.
- Min, K., et al. (2000), A test for systematic errors in <sup>40</sup>Ar/<sup>39</sup>Ar geochronology through comparison with U/Pb analysis of a 1.1-Ga rhyolite, *Geochim. Cosmochim. Acta*, 64(1), 73–98, doi:10.1016/S0016-7037(99)00204-5.
- Montanez, I. P., et al. (2007), CO<sub>2</sub>-forced climate and vegetation instability during late Paleozoic deglaciation, *Science*, 315(5808), 87–91, doi:10.1126/science.1134207.
- Mundil, R., et al. (2004), Age and timing of the end Permian mass extinctions: U/Pb geochronology on closed-system zircons, *Science*, 305, 1760–1763, doi:10.1126/science.1101012.
- Nemirovskaya, T. I., et al. (1990), The Kal'mius section, Donbass, Ukraine, U.S.S.R.: A Soviet proposal for the Mid-Carboniferous boundary stratotype, *Courier Forsch. Senckenberg*, 130, 247–272.
- Nemirovskaya, T. I., et al. (1994), *Lochriea zieglerei* and *Lochriea senckenbergica*—New conodont species from the latest Viséan and Serpukhovian in Europe, *Courier Forsch. Senckenberg*, 168, 311–317.
- Nemyrovskaya, T. I. (1999), Bashkirian conodonts of the Donets Basin, Ukraine, *Scr. Geol.*, 119, 1–115.
- Nemyrovskaya, T. I., et al. (1999), On Moscovian (Late Carboniferous) conodonts of the Donets Basin, Ukraine, *Neues Jahrb. Geol. Palaeontol. Abh.*, 214(1–2), 169–194.
- Nikitin, S. N. (1890), *Kamennougol'nye otlozheniya podmoskovnogo kraya i artesijskie vody pod Moscovoi (Carboniferous Deposits of Moscow Basin and Artesian Water Around Moscow)*, 138 pp., Geol. Comm. of Russ., Saint Petersburg.
- Nikolaeva, S. V., L. Z. Akhmetshina, V. A. Konovalova, V. F. Korobkov, and G. F. Zainakaeva (2009), The Carboniferous carbonates of the Dombar Hills (western Kazakhstan) and the problem of the Viséan-Serpukhovian boundary, *Palaeoworld*, 18(2–3), 80–93.
- Pazukhin, V. N., A. S. Aleksev, N. V. Goreva, and E. I. Kulagina (2006), Discovery of potential Bashkirian-Moscovian boundary marker conodont *Declinognathodus donetzianus* in south Urals, *Newsl. Carboniferous Stratigr.*, 24, 18–19.
- Poletaev, V. I. (1981), *Lithostratigraphic Subdivisions the Carbonate Sequences of Lower Carboniferous in Donets Basin*, 49 pp., Geol. Inst., Ukrainian Acad. of Sci., Kiev.
- Poletaev, V. I., et al. (1991), Local zones and major Lower Carboniferous biostratigraphic boundaries of the Donets Basin (Donbass), Ukraine, U.S.S.R., *Courier Forsch. Senckenberg*, 130, 47–59.
- Popov, A. V. (1979), Kamennougol'nyye ammonoidei Donbassa i ikh stratigraficheskoye znachenie (Carboniferous Ammonoidea of the Donets Basin and Their stratigraphic significance), *Tr. Vses. Ordena Lenina Nauchno Issled. Geol. Inst. im A.P. Karpinskogo, Novaya Ser.*, 220, 106 pp.
- Poty, E., et al. (2006), Upper Devonian and Mississippian foraminiferal and rugose coral zonations of Belgium and northern France: A tool for Eurasian correlations, *Geol. Mag.*, 143(6), 829–857, doi:10.1017/S0016756806002457.
- Poulsen, C. J., et al. (2007), Late Paleozoic tropical climate response to Gondwanan deglaciation, *Geology*, 35(9), 771–774, doi:10.1130/G23841A.1.
- Putrja, F. S. (1948), *Protriticites*—A new genus of fusulinids (in Russian), *Trans. L'vov Geol. Soc., Ser. Paleontol.*, 1, 89–96.
- Ramezani, J., et al. (2007), High-precision U-Pb zircon age constraints on the Carboniferous-Permian boundary in the southern Urals stratotype, *Earth Planet. Sci. Lett.*, 256(1–2), 244–257, doi:10.1016/j.epsl.2007.01.032.
- Rasbury, E. T., et al. (1998), U-Pb dates of paleosols: Constraints on late Paleozoic cycle durations and boundary ages, *Geology*, 26, 403–406, doi:10.1130/0091-7613(1998)026<0403:UPDOPC>2.3.CO;2.
- Rauscher-Chernousova, D. M. (1941), New Upper Carboniferous stratigraphic data from the Oksko-Tsinnitskiy Dome (in Russian), *Rep. Acad. Sci. USSR*, 30(5), 434–436.
- Rauscher-Chernousova, D. M., and E. A. Reitlinger (1954), Biostratigraphic distribution of foraminifers in Middle Carboniferous deposits of southern limb of Moscow Syncline (in Russian), in *Regional Stratigraphy of the U.S.S.R.*, vol. 2, *Stratigraphy of Middle Carboniferous Deposits of Central and Eastern Parts of Russian Platforms (Based on Foraminifers Study)*. 1. *Moscow Syncline*, edited by D. V. Nalivkin and V. V. Menner, *Tr. Akad. Nauk SSSR Geol. Inst.*, 7–120.
- Renne, P. R., et al. (1998), Intercalibration of standards, absolute ages and uncertainties in <sup>40</sup>Ar/<sup>39</sup>Ar dating, *Chem. Geol.*, 145, 117–152, doi:10.1016/S0009-2541(97)00159-9.
- Ritter, S. M. (1995), Upper Missourian-Lower Wolfcampian (Upper Kasimovian-Lower Asselian) conodont biostratigraphy



- phy of the midcontinent, USA, *J. Paleontol.*, **69**, 1139–1154.
- Ross, C. A., and J. R. P. Ross (1988), Late Paleozoic transgressive-regressive deposition, in *Sea-Level Changes—An Integrated Approach*, edited by C. K. Wilgus et al., *Spec. Publ. Soc. Econ. Paleontol. Mineral.*, **42**, 227–247.
- Rotai, A. P. (1975), Donets Basin (in Russian), in *Main Features of Carboniferous of USSR*, edited by A. P. Rotai, pp. 80–101, Nauka, Saint Petersburg, Russia.
- Rozovskaya, S. E. (1950), *Rod Triticites, ego razvitie i stratigraficheskoe znachenie (Triticites Genus: Its Evolution and Stratigraphic Significance)*, 80 pp., *Tr. Paleontol. Inst.*, **26**, 80 pp.
- Savchuk, S. V. (1957), K voprosu o promyshlennoi klassifikatsii nizhnekarbonovykh uglei Donbassa, *Izv. Dnepropetr. Gorn. Inst.*, **29**, 47–65.
- Schellwien, E. (1908), Monographie der Fusulinen. Teil I: Die Fusulinen des russisch-arktischen Meeresgebietes, *Palaeontographica*, **55**, 145–194.
- Schmitz, M. D., and B. Schoene (2007), Derivation of isotope ratios, errors, and error correlations for U-Pb geochronology using <sup>205</sup>Pb-<sup>235</sup>U- (<sup>233</sup>U)-spiked isotope dilution thermal ionization mass spectrometric data, *Geochem. Geophys. Geosyst.*, **8**, Q08006, doi:10.1029/2006GC001492.
- Schmitz, M. D., et al. (2005), New ID-TIMS U-Pb zircon ages for the Carboniferous-Permian boundary sections of the southern Urals–Russia, Kazakhstan, *Geochim. Cosmochim. Acta*, **69**(10), suppl., 326.
- Shchegolev, A. K. (1975), Die Entwicklung der Pflanzenbedeckung im Sueden des Europaeischen Teils der UdSSR, vom Ende des Mittelkarbons bis zum Perm; Umfang und Gliederung des oberen Karbons (Stefan) (The evolution of the vegetation in the south of the European USSR, from the end of the middle Carboniferous to the Permian: Extent and stratigraphic divisions of the upper Carboniferous or Stephanian), *C. R. Congr. Int. Stratigr. Geol. Carbonifere*, **4**(7), 275–280.
- Shchegolev, A. K., and R. I. Kozitskaya (1984), The paleontological basis of the project of the Upper Carboniferous standard scale in the Europe and the central Asia (in Russian), in *The Upper Carboniferous of the USSR*, edited by V. V. Menner and A. D. Grigor'yeva, pp. 107–113, Nauka, Moscow.
- Skompski, S., et al. (1995), Conodont distribution across the Viséan/Namurian boundary, *Courier Forsch. Senckenberg*, **188**, 177–209.
- Somerville, I. D. (2008), Biostratigraphic zonation and correlation of Mississippian rocks in western Europe: Some case studies in the late Viséan/Serpukhovian, *Geol. J.*, **43**(2–3), 209–240, doi:10.1002/gj.1097.
- Soreghan, G. S., and W. R. Dickinson (1994), Generic types of stratigraphic cycles controlled by eustasy, *Geology*, **22**(8), 759–761, doi:10.1130/0091-7613(1994)022<0759:GTOSCC>2.3.CO;2.
- Soreghan, G. S., and K. A. Giles (1999), Amplitudes of Late Pennsylvanian glacioeustasy, *Geology*, **27**(3), 255–258, doi:10.1130/0091-7613(1999)027<0255:AOLPG>2.3.CO;2.
- Stovba, S. M., and R. A. Stephenson (1999), The Donbas Foldbelt: Its relationships with the uninverted Donets segment of the Dniepr-Donets Basin, Ukraine, *Tectonophysics*, **313**(1–2), 59–83, doi:10.1016/S0040-1951(99)00190-0.
- Stovba, S. M., et al. (1996), Structural features and evolution of the Dnieper-Donets Basin, Ukraine, from regional seismic reflection profiles, *Tectonophysics*, **268**, 127–147, doi:10.1016/S0040-1951(96)00222-3.
- Tschernyshev, F. N., and L. I. Lutugin (1897), Donets Basin (in Russian), *News Soc. Min. Eng.*, no. 11–12, 15–40.
- Vdovenko, M. V. (1954), New species of Foraminifers from the Lower Viséan of the Donets Basin (in Russian), *Sci. Notes Kiev Univ.*, **13**(4), 63–76.
- Vdovenko, M. V. (2001), Atlas of foraminifera from the upper Viséan and lower Serpukhovian (Lower Carboniferous) of the Donets Basin (Ukraine), *Abh. Ber. Nat.*, **23**, 93–178.
- Vdovenko, M. V., et al. (1990), An overview of Lower Carboniferous biozones of the Russian Platform, *J. Foraminiferal Res.*, **20**(3), 184–194, doi:10.2113/gsjfr.20.3.184.
- Villa, E. and the Task Group (2008), Progress Report of the Task Group to establish the Moscovian-Kasimovian and Kasimovian-Gzhelian boundaries, *Newsl. Carboniferous Stratigr.*, **26**, 12–13.
- Villeneuve, M., et al. (2000), A method for intercalibration of U-Th-Pb and <sup>40</sup>Ar-<sup>39</sup>Ar ages in the Phanerozoic, *Geochim. Cosmochim. Acta*, **64**(23), 4017–4030, doi:10.1016/S0016-7037(00)00484-1.
- Wang, Z., et al. (2007), Conodont sequence across Bashkirian-Moscovian boundary in the Nashui Section, Luodian, Guizhou, south China, *J. Stratigr.*, **31**(1), 102–103.
- Wanless, H. R., and F. P. Shepard (1936), Sea level and climatic changes related to late Paleozoic cycles, *Geol. Soc. Am. Bull.*, **47**(8), 1177–1206.
- Wardlaw, B. R., et al. (2004), The Permian period, in *A Geologic Time Scale 2004*, edited by F. M. Gradstein et al., pp. 249–270, Cambridge Univ. Press, Cambridge, U. K.
- Zaritskiy, P. V. (1977), Kaolinite partings in coal of the Donets Basin, *Lithol. Miner. Resour.*, **12**(6), 725–729.
- Zhemchuzhnikov, Y. A., and V. S. Yablokov (1956), Fatsialno-tsiklicheskiy metod izucheniya uglenosnykh otlozhenii (in Russian), *Tr. Lab. Geol. Uglya Akad. Nauk SSSR*, **5**, 161–170.